MULTI-TEMPORAL TERRESTRIAL LIDAR FOR ESTIMATING INDIVIDUAL TREE DIMENSIONS AND BIOMASS CHANGE

A Thesis

by

SHRUTHI SRINIVASAN

Submitted to the Office of Graduate and Professional Studies of
Texas A&M University
in partial fulfillment of the requirements for the degree of

MASTER OF SCIENCE

Chair of Committee,	Sorin C. Popescu
Committee Members,	Marian Eriksson
	Anthony M. Filippi
Head of Department,	David D. Baltensperger

December 2013

Major Subject: Ecosystem Science and Management

ABSTRACT

Accurate measures of forest structural parameters are essential to forest inventory and growth models, managing wildfires, and modeling of carbon cycle. Terrestrial laser scanning (TLS) provides accurate understory information rapidly through non-destructive methods. This study developed algorithms to extract individual tree height, diameter at breast height (DBH), and crown width in plots at Ecosystem Science and Management (ESSM) research area and Huntsville, Texas. Further, the influence of scan settings and processing choices on the accuracy of deriving tree measurements was also investigated. The study also developed models to estimate aboveground biomass (AGB) and investigate different conceptual approaches to study tree level growth in forest structural parameters and AGB using multi-temporal TLS datasets.

DBH was retrieved by cylinder fitting at different height bins. Individual trees were extracted from the TLS point cloud to determine tree heights and crown widths. The R-squared value ranged from 0.91 to 0.97 when field measured DBH was validated against TLS derived DBH using different methods. An accuracy of 92% was obtained for predicting tree heights. The R-squared value was 0.84 and RMSE was 1.08 m when TLS derived crown widths were validated using field measured crown widths. Examples of underestimations of field measured forest structural parameters due to tree shadowing have also been discussed in this study. Correction factors should be applied or multiple high resolution scans should be conducted to reduce the errors in estimation of forest structural parameters.

TLS geometric and statistical parameters were derived for individual trees and used as explanatory variables to estimate AGB. An extensive literature review reveals that this is the first study to model the change in AGB using different innovative and conceptual approaches with multi-temporal TLS data. Tree level AGB growth was studied over a period of three years using three different approaches. Results showed that TLS derived geometric parameters were better correlated to field measured AGB. Promising results for AGB change were obtained using the direct modeling approach; hence forest growth could be studied independent of any field measurements when biomass models are available. However, the models could be improved by incorporating more trees with a wide range of DBH and tree heights. The results from this study will benefit foresters, planners, and other remote sensing studies from airborne and spaceborne platforms, for map upscaling, data fusion, or calibration purposes.

DEDICATION

To my parents, Meena and Srinivasan, and sister Preethi

ACKNOWLEDGEMENTS

I would like to express my sincere gratitude to my committee chair and advisor, Dr.Sorin C. Popescu for the continuous support of my Master's study and research. Without his constant guidance and encouragement throughout the course of my study, this thesis would have not been possible. His continued motivation inspired me to present my research at several conferences. I sincerely hope to learn from him throughout my career.

A special thanks to my committee members, Dr. Marian Eriksson and Dr. Anthony Filippi for their time, advice and valuable feedback. I am also grateful to Dr. Robert A. Washington-Allen and Dr. David D. Briske for their warm encouragement.

My heartfelt appreciations go to Ryan D. Sheridan and Nian-Wei Ku for providing insightful comments and suggestions throughout my research work and assisting with field data collection. I am fortunate to have spent a wonderful time in a friendly working environment at the Spatial Science Laboratory. I am also thankful to Dr. Kaiguang Zhao, Ohio State University, Dr. Muge Agca, Aksaray University, and Jared Stukey for their help with field data collection.

I have greatly benefited from the financial support I received from various sources, including the Department of Ecosystem Science and Management and College of Agriculture and Life Sciences Excellence Fellowship and graduate student support.

Finally, I would like to thank my parents and sister for their moral support and encouragement throughout my graduate career.

NOMENCLATURE

AGB	Aboveground Biomass
AGL	Above Ground Level
ASCII	American Standard Code for Information Interchange
CBH	Crown Base Height
CSV	Comma Separated Value
CW	Crown Width
DBH	Diameter at Breast Height
DEM	Digital Elevation Model
ESSM	Ecosystem Science and Management
GPS	Global Positioning System
HOME	Height Of Median Energy
LAS	LASer
LDV	Lidar Data Viewer
LTI	Laser Technology Inc
MAD	Median Absolute Deviation
NA	Not Available
NAIP	National Agriculture Imagery Program
QTM	Quick Terrain Modeler
RMSE	Root Mean Square Error
TLS	Terrestrial Laser Scanning

TreeVaW	Tree Variable Window
VIF	Variance Inflation Factor
WAAS	Wide Area Augmentation System

TABLE OF CONTENTS

Page

LIST OF FIGURES

Page

LIST OF TABLES

Page

CHAPTER I

INTRODUCTION AND LITERATURE REVIEW

Accurate measures of forest structural parameters and monitoring their changes though time are essential to forest inventory and growth models, managing wildfires, modeling of carbon cycle, and forest management systems (Næsset *et al*., 2004). Most extant methods, which include indirect and direct measurement techniques, are limited in their capability to acquire accurate, spatially explicit measurements of forest three-dimensional structural parameters. The accuracy of these measurements can be improved using lidar (light detection and ranging) (Kussner and Mosandl, 2000; Henning and Radtke, 2006).

Lidar, which is an active sensor, emits a series of laser pulses and measures the distance to targets using the speed of light and travel time of the laser pulses to and from a system (Lefsky *et al*., 2002a). Unlike passive optical remote sensing, lidar remote sensing provides detailed information on both horizontal and vertical distribution of vegetation in forests (Lim *et al*., 2003). Applications of lidar remote sensing such as measurement of the structure and function of vegetation canopies and estimation of tree height, crown width, basal area, stem volume, and aboveground biomass (AGB) are elaborated in various studies (Lefsky *et al*., 2002b; Chen *et al*., 2007; Popescu and Zhao, 2008; Falkowski *et al*., 2009). Non-destructive measurements of AGB can be done using airborne lidar with a higher accuracy compared to AGB measurements obtained through other remote sensing techniques (Lefsky *et al*., 2002a; Bortolot and Wynne, 2005;

Popescu, 2007; Hudak *et al*., 2012). Nevertheless, tree height estimates with small footprint discrete return airborne lidar tend to slightly underestimate manual measurements done in the field, as the laser pulses are not always reflected from tree tops. Airborne lidar may not capture the complete vertical distribution of the canopy (Lim *et al*., 2003). Terrestrial laser scanning (TLS) fills the gap between tree scale manual measurements and large scale airborne lidar measurements by providing a wealth of precise information on various forest structural parameters (Maas *et al*., 2008; Dassot *et al*., 2011) and a digital record of the three-dimensional structure of forests at a given time. Hence, to obtain accurate understory information and detailed canopy vertical structure depiction, TLS can produce better results when compared to airborne lidar and field measurements (Loudermilk *et al*., 2009).

The use of terrestrial or ground-based laser scanners for forest management planning and mapping vegetation properties has grown dramatically in the last decade (Moskal *et al*., 2009; Moskal and Zheng, 2012; Kankare *et al*., 2013). Terrestrial laser scanners have a high potential to acquire three-dimensional data of standing trees accurately and rapidly through non-destructive methods, which has resulted in the multiple use of this technology in studying forest environments (Lovell *et al*., 2003; Dassot *et al*., 2011). Several studies have shown that TLS is a promising technology in providing objective measures of tree height, diameter at breast height (DBH), stem density, canopy cover, and AGB (Bienert *et al*., 2006; Hopkinson *et al*., 2008; Maas *et al*., 2008; Kankare *et al*., 2013). However, a drawback of this technology is the inability of the laser pulses to penetrate through the trees if they are shadowed by other branches,

stems or understory (occlusion or shadowing), which finally leads to the underestimation of field measured parameters (Bienert *et al*., 2006; Van Der Zande *et al*., 2006; Moskal and Zheng, 2012).

Among the various forest measurements, DBH or stem diameter is an important forest inventory attribute because it serves as a fundamental parameter in tree allometry and estimation of basal area, thus providing valuable information about individual trees and forest stand structure (Moskal and Zheng, 2012). The automatic detection of DBH from TLS data has been investigated in various studies. For example, Huang et al. (2009) implemented a circle approximation to retrieve DBH, and they concluded that the circle fitting algorithm resulted in a smaller diameter when there were insufficient surface laser points. Hopkinson et al. (2004) estimated DBH by fitting a cylinder primitive to the TLS data. Stems with sparse points were omitted from the analysis. Though the residual dispersion was greater in homogenous plantations, the authors achieved an overall significant correlation with an R-squared value of 0.85 between lidar and field measurements for DBH. Bienert et al. (2006) determined DBH efficiently using a circle fitting algorithm, and they added that DBH measurements from TLS could be fraught with errors if adequate laser points are not available due to occlusion from other stems. Watt and Donoghue (2005) concluded that accurate DBH measurements from TLS datasets can be obtained only for unobstructed trees. The previously mentioned studies indicate that TLS can be used to accurately measure individual tree attributes, such as DBH, in datasets with sufficient stem returns. However, no research has been done on retrieving DBH using cylinder fitting with different height bins to

account for sparse laser points (Aschoff and Spiecker, 2004; Bienert *et al*., 2006; Mass *et al*., 2008; Huang *et al*., 2009).

In addition to DBH, tree height is also a vital parameter that provides qualitative information about the plot or stand and quantitative information about the tree. Tree height is strongly related to various biophysical characteristics and is a function of species composition and climate quality. DBH and tree heights are positively correlated with biomass, since stem diameter increases as trees grow taller, thus increasing the amount of foliage supported by the trees (Dubayah and Drake, 2000). A variety of studies have successfully retrieved tree heights using terrestrial laser scanners (Huang *et al*., 2009; Moskal and Zheng, 2012). Hopkinson et al. (2004) determined tree heights from terrestrial lidar data by fitting vector primitives, and their findings revealed that TLS derived tree heights underestimated field measurements by approximately 1.5 m. This underestimation was due to the reduced lidar point density in upper canopy, a direct result of the occlusion caused by lower canopy and position of the sensor. The results were also justified by a weak relationship illustrated between TLS and field measured heights for taller trees. Chasmer et al. (2006) compared field measured heights and TLS derived heights for 15 trees. Their results indicated that TLS derived heights underestimated field measured heights by an approximately 1.2 m due to reduced penetration of laser pulses within the lower canopy because of occlusion by other trees. Van Der Zande et al. (2006) illustrated that terrestrial lidar point density is negatively correlated with heights in plots with minimal understory. Thus, a few tree tops might be missed by laser hits due to shadowing, which further underestimates various lidar

derived height metrics. Huang et al. (2009) demonstrated an automatic method to determine tree heights from TLS data, and they achieved a correlation of 0.95 for TLS derived tree heights and field measured heights. Moskal and Zheng (2012) estimated tree heights in heterogeneous stands using TLS data by calculating the difference between the lowest and the highest slice plane from horizontal point cloud slicing. Due to occlusion effects, the laser pulses could not penetrate fully through the complex canopy to reach the top of trees and accounted for only 57.27% accuracy in predicting tree heights.

Crown width (CW) is an important variable, which can be used to estimate biomass, tree volume, and leaf area (Evans *et al*., 2006). An extensive literature study reveals that crown width has so far not been estimated from TLS data and a limited number of studies have derived crown width from airborne lidar data. Relationships between airborne lidar and field derived crown dimensions are significant, but not very strong, with R-squared values ranging from 0.51 to 0.63 (Naesset and Oakland, 2002; Popescu *et al*., 2003; Evans *et al*., 2006; Van Leeuwen and Nieuwenhuis, 2010). A significant parameter in the indirect measurement of true leaf area index is gap fraction (Danson *et al*.; 2007). The authors determined stand-level directional gap fraction distributions using TLS and found the results were similar to gap fraction measurements obtained from hemispherical photographs. Crown cover is another essential attribute, which is used to measure tree health, and it is an approximate indicator of stand density (Avery and Burkhart, 2002). It provides information on the amount of plant material,

such as leaves and branches that obstructs sunlight from penetrating through the tree crown.

AGB is defined as all the living biomass above the soil that includes stem, stump, branches, bark, seeds, and foliage; it is associated with important components such as tree health, forest regeneration, and energy conversion (Jenkins *et al*., 2003). It is a crucial ecological variable, which has to be accurately estimated to reduce the uncertainties in the estimates of forest carbon budget and understand potential changes of the climate system. Further, half of the dry biomass is considered to account for carbon, which is of great scientific interest to understand the carbon cycle (Houghton *et al*., 2009; Lin *et al*., 2010; Zolkos *et al*., 2013). Næsset et al. (2011) developed non-linear biomass models using airborne lidar derived height metrics and canopy density. The authors performed a stepwise forward selection procedure to select the best set of independent variables to estimate biomass. They observed that the estimated biomass was not statistically different from field measured biomass for lidar based models. Yao et al. (2011) used a ground-based, scanning near-infrared full waveform lidar and retrieved tree diameters and stem count density to determine aboveground standing biomass. They obtained a coefficient of determination of 0.85 between the lidar derived and field measured biomass. Lefsky et al. (2002b) developed a single equation to estimate AGB from lidar derived canopy structure in three distinct study sites that explained 84% of the variance. Zolkos et al. (2013) combined and contrasted results from different studies on the estimation of AGB from lidar remote sensing and found that AGB estimated from remote sensing models were closely related to field measured

AGB if the residual standard error was less than or equal to 20 Mg ha^{-1}. They also discussed that significantly better results for the estimation of AGB were obtained using airborne lidar data compared to radar or optical data. However, very little research has been done in estimating AGB at individual tree level with TLS data, which could be used in the detailed evaluation of silvicultural techniques (Kankare *et al*., 2013).

Evans et al. (2006) addressed the use of lidar for forest assessments and proposed two significant domains in which lidar could be a major contributor: (1) tree growth and yield modelling at individual tree level for pine plantations using multi-temporal lidar data; and (2) implementation of the retrieved individual tree measurements from lidar data in immersive visualization environments for the assessment of forest stands. Lidar is a promising technology to study growth and derive forest parameters (Hudak *et al*., 2009). Few studies have investigated forest succession using lidar to predict long-term carbon sequestration (Falkowski *et al*., 2009; Hudak *et al*., 2012). Successful modeling of change in airborne lidar estimated biomass has been done using three different approaches: (1) computing the change in biomass by subtracting the estimated biomass between two different years; (2) modeling of biomass change by a system of models; and (3) direct modeling of biomass change (Bollandsås *et al*., 2013). Hopkinson et al. (2008) assessed the plot level mean tree height growth for homogenous red pine conifer plantations over a five period using repeat airborne lidar datasets. They found that lidar estimated growth rates slightly underestimated the field measured growth rates. Falkowski et al. (2009) mapped forest succession using lidar metrics with an overall accuracy higher than 90%. Hudak et al. (2012) quantified AGB due to forest growth

using repeat airborne lidar surveys. They developed predictive tree AGB models using random forest algorithm and monitored biomass change using repeat discrete return airborne lidar and field surveys. They reported mean canopy height as the most significant predictor for tree biomass. Though their results suggested that biomass change and carbon dynamics in conifer forests were monitored efficiently with discrete return multi-temporal airborne lidar datasets, a few challenges concerning repeated measures using airborne lidar exist, such as differences in lidar acquisition pulse density. Yu et al. (2006) were able to measure four years of height growth of 82 Scots pines *(Pinus sylvestris)* with multi-temporal laser surveys, and they developed a tree-to-tree matching algorithm. The three change detection techniques used in their study were: (1) differencing between canopy height models; (2) comparison between canopy profile, and (3) analysis of difference between height histograms. An R-squared value of 0.68 was obtained when field measured individual tree height growth was validated against laser derived individual tree height growth. However, multi-temporal airborne laser scans poses some difficulties such as changes in flight conditions and flight path. Though very limited research has been done on AGB change estimation using lidar, several authors have discussed the potential of this technology to study forest growth (Yu *et al*., 2006; Næsset *et al*., 2013). Situations where airborne laser data cannot be used for change detection studies are described by the previously mentioned authors, and they suggest the use of TLS for future growth analysis.

The use of TLS for spatially explicit assessment of plot level forest canopy structure was examined by Henning and Radtke (2006) in leaf-off and leaf-on

conditions. The authors quantified differences in characterizations obtained under the two conditions. The comparison results of leaf-on and leaf-off provided a RMSE of 0.169 m in DBH and mean position error of 0.29 m. Their results support the applications of TLS for multi-temporal observation. However, registration of TLS data across time was not studied by the authors, but when performed could prove advantageous for multi-temporal change detection. Kaasalainen et al. (2010) and Kankare et al. (2013) analyzed the potential of TLS to measure standing tree biomass in a laboratory environment. One main drawback of local scale AGB estimates produced using field measurements or low resolution satellite imagery are the estimate uncertainties. However, TLS data allows for non-destructive and detailed modeling of individual trees. For example, Kankare et al. (2013) developed single tree based AGB models from multiple scan TLS data and reported improved accuracies for branch biomass. They input 83 TLS based variables and performed lasso regression and stepwise regression to estimate biomass. Kaasalainen et al. (2010) concluded that TLS is a promising technology for studying biomass change, and they obtained high R-squared values of 0.95 to 0.99 when TLS estimated standing tree biomass were validated with field measured biomass.

The majority of existing studies only investigate biomass estimation in static conditions, i.e., determining various forest parameters and estimating AGB at a single point in time. Thus, by utilizing multi-temporal lidar data, there is potential in increasing the scope of lidar remote sensing for carbon modeling, wildfire risk assessment, and other applications (Hudak *et al*., 2009). Biomass is dynamic and hence has to be

monitored continuously to provide information on sinks and sources of carbon. It is also essential to utilize such information to project AGB changes to inform decision making processes (Avery and Burkhart, 2002; Houghton *et al*., 2009).

Until recently, measuring and monitoring forest growth were mostly done using airborne laser scanning, making retrieval of forest attributes and change detection challenging at the individual tree level. Since the potential to retrieve different forest structural parameters and monitor forest growth using multi-temporal TLS data is not completely tested in the current literature, this study will investigate methods to measure and monitor tree level forest structural parameters and AGB, which will benefit forest management and other remote sensing studies from airborne and spaceborne platforms, for map upscaling, data fusion, or calibration purposes.

Since Southern pine forests are extremely productive and bolster forest carbon sequestration capacity, regular monitoring of forests is essential to foresters and planners for managing forest resources and ecosystem services efficiently (Johnsen *et al*., 2001). As the non-destructive and non-contact measurements can be collected by a lidar system at multiple moments in time, the growth parameters of trees over time can be assessed (Watt and Donoghue, 2005; Dassot *et al*., 2011) with high accuracy. In addition, when extended to a larger area, the multi-temporal change study will provide us with information on tree mortality and continuous forest dynamics.

The overall aim of this study is to develop a methodology to retrieve tree level forest structural parameters and AGB and study tree level growth using multi-temporal TLS datasets. Specific objectives are to 1) develop methods to estimate tree height,

DBH, and crown width from TLS datasets at individual tree level; 2) investigate the influence of scan settings, such as leaf-on/leaf-off seasons, tree positioning relative to scanner, and processing choices, on the accuracy of deriving tree measurements; (3) develop models using TLS parameters to estimate tree level AGB; and (4) investigate different conceptual approaches for estimating change in AGB with multi-temporal lidar scans.

This thesis is organized into four major sections. An overall introduction and literature review are presented in chapter I. Chapters II and III follow the style of individual manuscripts. Overall summary and conclusions for this study are discussed in chapter IV.

CHAPTER II

TERRESTRIAL LIDAR AS AN EFFECTIVE TOOL TO RETRIEVE TREE LEVEL HEIGHT, CROWN WIDTH, AND STEM DIAMETER

2.1 Introduction

Accurate measures of forest structural parameters and monitoring their changes though time are essential to forest inventory and growth models, managing wildfires, modeling of carbon cycle, and forest management systems (Næsset *et al*., 2004). Most extant methods, which include indirect and direct measurement techniques, are limited in their capability to acquire accurate, spatially explicit measurements of forest three-dimensional structural parameters. The accuracy of these measurements can be improved using lidar (light detection and ranging) (Kussner and Mosandl, 2000; Henning and Radtke, 2006).

Lidar, which is an active sensor, emits a series of laser pulses and measures the distance to targets using the speed of light and travel time of the laser pulses to and from a system (Lefsky *et al*., 2002a). Unlike passive optical remote sensing, lidar remote sensing provides detailed information on both horizontal and vertical distribution of vegetation in forests (Lim *et al*., 2003). Applications of lidar remote sensing such as measurement of the structure and function of vegetation canopies and estimation of tree height, crown width, basal area, stem volume, and aboveground biomass are elaborated in various studies (Lefsky *et al*., 2002b; Chen *et al*., 2007; Popescu and Zhao, 2008; Falkowski *et al*., 2009). Nevertheless, tree height estimates with small footprint discrete

return airborne lidar tend to slightly underestimate manual measurements done in the field, as the laser pulses are not always reflected from tree tops. Airborne lidar may not capture the complete vertical distribution of the canopy (Lim *et al*., 2003). Terrestrial laser scanning (TLS) fills the gap between tree scale manual measurements and large scale airborne lidar measurements by providing a wealth of precise information on various forest structural parameters (Maas *et al*., 2008; Dassot *et al*., 2011) and a digital record of the three-dimensional structure of forests at a given time. Hence, to obtain accurate understory information and detailed canopy vertical structure depiction, TLS can produce better results when compared to airborne lidar and field measurements (Loudermilk *et al*., 2009).

The use of terrestrial or ground-based laser scanners for forest management planning and mapping vegetation properties has grown dramatically in the last decade (Moskal *et al*., 2009; Moskal and Zheng, 2012; Kankare *et al*., 2013). Terrestrial laser scanners have a high potential to acquire three-dimensional data of standing trees accurately and rapidly through non-destructive methods, which has resulted in the multiple use of this technology in studying forest environments (Lovell *et al*., 2003; Dassot *et al*., 2011). Several studies have shown that TLS is a promising technology in providing objective measures of tree height, diameter at breast height (DBH), stem density, canopy cover, and plot level volumes (Hopkinson *et al*., 2004; Bienert *et al*., 2006; Maas *et al*., 2008). However, a drawback of this technology is the inability of the laser pulses to penetrate through the trees if they are shadowed by other branches, stems or understory (occlusion or shadowing), which finally leads to the underestimation of

field measured parameters (Bienert *et al*., 2006; Van Der Zande *et al*., 2006; Moskal and Zheng, 2012).

Among the various forest measurements, DBH or stem diameter is an important forest inventory attribute because it serves as a fundamental parameter in tree allometry and estimation of basal area, thus providing valuable information about individual trees and forest stand structure (Moskal and Zheng, 2012). The automatic detection of DBH from TLS data has been investigated in various studies as listed in table 1. For example, Huang et al. (2009) implemented a circle approximation to retrieve DBH, and they concluded that the circle fitting algorithm resulted in a smaller diameter when there were insufficient surface laser points. Hopkinson et al. (2004) estimated DBH by fitting a cylinder primitive to the TLS data. Stems with sparse points were omitted from the analysis. Though the residual dispersion was greater in homogenous plantations, the authors achieved an overall significant correlation with an R-squared value of 0.85 between lidar and field measurements for DBH. Bienert et al. (2006) determined DBH efficiently using a circle fitting algorithm, and they added that DBH measurements from TLS could be fraught with errors if adequate laser points are not available due to occlusion from other stems. Watt and Donoghue (2005) concluded that accurate DBH measurements from TLS datasets can be obtained only for unobstructed trees. The previously mentioned studies indicate that TLS can be used to accurately measure individual tree attributes, such as DBH, in datasets with sufficient stem returns. However, no research has been done on retrieving DBH using cylinder fitting with different height bins to account for sparse laser points (Table 1).

Table 1. Overview of DBH retrieval methods using TLS datasets and their results.

Reference	DBH retrieval method	Number of trees measured	Number of scans conducted	Results
Aschoff and Spiecker (2004)	Circle fitting at 1.2 m, 1.3 m and 1.4 m AGL	NA	Single scan and multiple scans (5 positions)	NA (not available)
Bienert et al. (2006)	Circle fitting at 1.3 m AGL	79	Single scan and multiple scans (3 positions)	Standard deviation ranged from1.21 to 2.47 cm
Brolly and Kiraly (2009)	(a) Single circle fitting at 1.3 m AGL (10 cm thickness)	154	Single scan	RMSE = 4.2 cm
	(b) Multiple circle fitting at 1 m, 1.5 m, 2 m AGL (10 cm thickness)	154	Single scan	RMSE = 3.4 cm
	(c) Cylinder fitting between 0.95 and 2.05 m AGL	134	Single scan	RMSE = 7.0 cm
Hopkinson et al. (2004)	Cylinder fitting between 1.25 and 1.75 m AGL	128	Multiple scans (5 positions)	$R^2 = 0.85$
Huang et al. (2009)	Circle fitting at 1.3 m AGL (10 cm thickness)	26	Multiple scans (4 positions)	$R^2 = 0.79$
Maas et al. (2008)	Circle fitting at 1.3 m AGL	80	Single scan and multiple scans (3 positions)	Overall RMSE = 1.8 cm
Tansey et al. (2009)	Circular Hough transformation for points between 1.27 and 1.33 m AGL, circle and cylinder fitting (0.04 m thick cross-section)	8	Multiple scans (4 positions)	RMSE ranged from 1.9 to 3.7 cm
Thies and Spiecker (2004)	Hough transformation and circle fitting at 1.3 m AGL	11	Single scan and multiple scans (4 positions)	NA
Watt and Donoghue (2005)	Circle fitting at 1.3 m AGL	12 (site 2)	Single scan at site 1 and multiple scans (2 positions) at site 2	$R^2 = 0.92$, site 2
Wezyk et al. (2007)	Cylinder fitting between 1.28 and 1.32 m AGL and pixel method	199	Multiple scans (4 positions)	$R^2 > 0.946$

*AGL - Above Ground Level, RMSE - Root Mean Square Error

In addition to DBH, tree height is also a vital parameter that provides qualitative information about the plot or stand and quantitative information about the tree. Tree height is strongly related to various biophysical characteristics and is a function of species composition and climate quality. DBH and tree heights are positively correlated with biomass, since stem diameter increases as trees grow taller, thus increasing the amount of foliage supported by the trees (Dubayah and Drake, 2000). A variety of studies have successfully retrieved tree heights using terrestrial laser scanners (Huang *et al*., 2009; Moskal and Zheng, 2012). Hopkinson et al. (2004) determined tree heights from terrestrial lidar data by fitting vector primitives, and their findings revealed that TLS derived tree heights underestimated field measurements by approximately 1.5 m. This underestimation was due to the reduced lidar point density in upper canopy, a direct result of the occlusion caused by lower canopy and position of the sensor. The results were also justified by a weak relationship illustrated between TLS and field measured heights for taller trees. Chasmer et al. (2006) compared field measured heights and TLS derived heights for 15 trees. Their results indicated that TLS derived heights underestimated field measured heights by an approximately 1.2 m due to reduced penetration of laser pulses within the lower canopy because of occlusion by other trees. Van Der Zande et al. (2006) illustrated that terrestrial lidar point density is negatively correlated with heights in plots that have zero or less understory. Thus, a few tree tops might be missed by laser hits due to shadowing, which further underestimates various lidar derived height metrics. Huang et al. (2009) demonstrated an automatic method to determine tree heights from TLS data, and they achieved a correlation of 0.95 for TLS

derived tree heights and field measured heights. Moskal and Zheng (2012) estimated tree heights in heterogeneous stands using TLS data by calculating the difference between the lowest and the highest slice plane from horizontal point cloud slicing. Due to occlusion effects, the laser pulses could not penetrate fully through the complex canopy to reach the top of trees and accounted for only 57.27% accuracy in predicting tree heights.

Crown width (CW) is an important variable, which can be used to estimate biomass, tree volume, and leaf area (Evans *et al*., 2006). An extensive literature study reveals that crown width has so far not been estimated from TLS data and a limited number of studies have derived crown width from airborne lidar data. Relationships between airborne lidar and field derived crown dimensions are significant, but not very strong, with R-squared values ranging from 0.51 to 0.63 (Naesset and Oakland, 2002; Popescu *et al*., 2003; Evans *et al*., 2006; Van Leeuwen and Nieuwenhuis, 2010). A significant parameter in the indirect measurement of true leaf area index is gap fraction (Danson *et al*.; 2007). The authors determined stand-level directional gap fraction distributions using TLS and found the results were similar to gap fraction measurements obtained from hemispherical photographs. Crown cover is another essential attribute, which is used to measure tree health, and it is an approximate indicator of stand density (Avery and Burkhart, 2002). It provides information on the amount of plant material, such as leaves and branches that obstructs sunlight from penetrating through the tree crown. Evans et al. (2006) addressed the use of lidar for forest assessments and proposed two significant domains in which lidar could be a major contributor: (1) tree growth and

yield modelling at individual tree level for pine plantations using multi-temporal lidar data; and (2) implementation of the retrieved individual tree measurements from lidar data in immersive visualization environments for the assessment of forest stands.

Until recently, measuring and monitoring forest growth were mostly done using airborne laser scanning, making retrieval of forest attributes and change detection challenging at the individual tree level. Since the potential to retrieve different forest structural parameters using TLS data is not completely tested in the current literature, this study will investigate methods to determine individual tree height, DBH, and crown width, which will benefit forest management and other remote sensing studies from airborne and spaceborne platforms, for map upscaling, data fusion, or calibration purposes. Since Southern pine forests are extremely productive and bolster forest carbon sequestration capacity, regular monitoring of forests is essential to foresters and planners for managing forest resources and ecosystem services efficiently (Johnsen *et al*., 2001).

The overall aim of this study is to develop innovative methods to retrieve forest structural parameters at individual tree level using lidar data sets acquired with TLS for two distinctly different study sites. Innovative aspects of our study consist in 1) developing new methods of deriving tree height, DBH, and crown width from TLS datasets at individual tree level; and 2) investigating the influence of scan settings, such as leaf-on/leaf-off seasons, tree positioning relative to scanner, and processing choices that affect DBH retrieval accuracy.

2.2 Materials and Methods

The flowchart presented in figure 1 shows the research methodology followed in this study. This section includes a description of the study area, data used for this study, TLS data processing, and the methods to extract individual trees and retrieve DBH, tree height, and crown width.

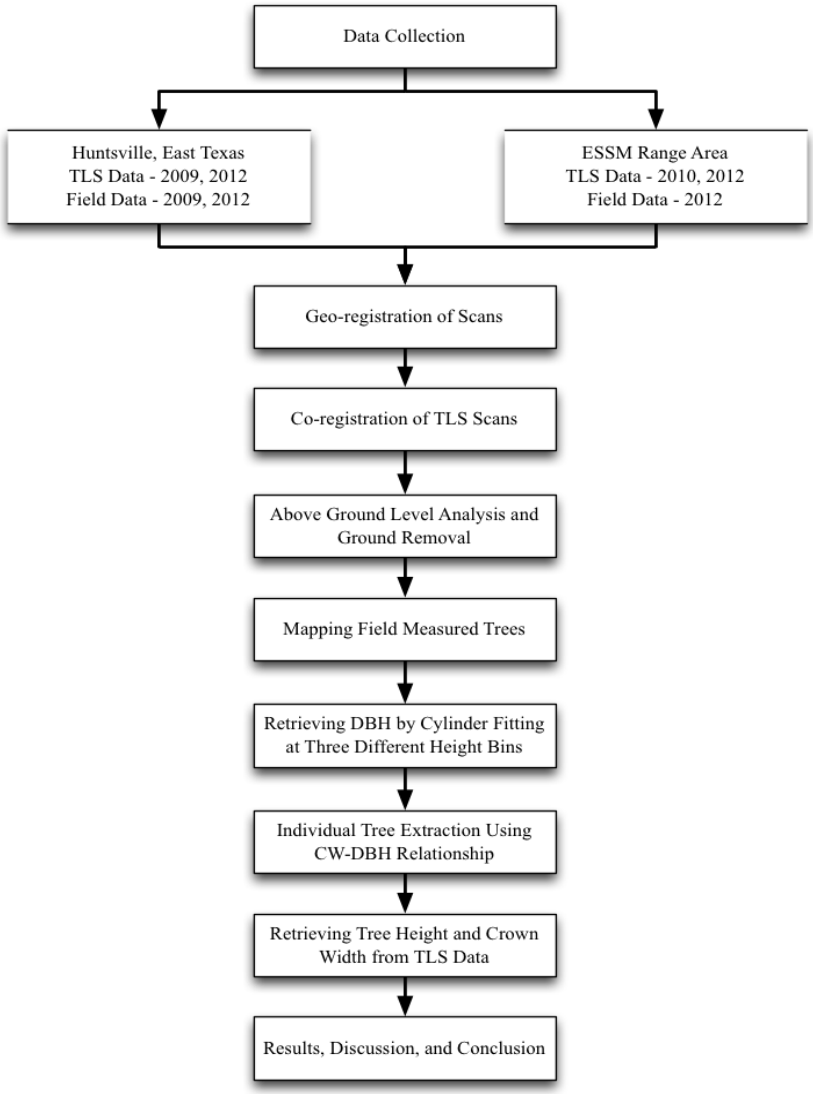

Figure 1. Methodology flowchart to retrieve tree height, DBH, and crown width.

2.2.1 Study Area

The study area for this research includes two different sites (Figure 2). Site 1, Ecosystem Science and Management (ESSM) range area, is located in College Station, TX, approximately 2.3 km south-east of Easterwood airport (30°34'25.95"N, 96°21'52.53"W). The study site covers an area of approximately 0.0012 km^2 and includes 21 post oak (*Quercus stellata*) trees. Post oak is a valuable contributor to the urban planting and wildlife food. The slope at this study site varies from 0 to 6 degrees, and the elevation ranges from 56.79 to 70.47 m. Site 2 is located near Huntsville, East Texas, centered within the rectangle defined by 95°24′57″W - 30°39′36″N and 95°21′33″W - 30°44′12″N. It includes seven circular plots; four plots cover an area of 404.600 m² (1/10th acre; r = 11.35 m) each and three plots cover an area of 40.468 m² (1/100th acre; r = 3.59 m) each. The dominant species in this site is loblolly pine (*Pinus taeda*), while other cover types in this area include upland and bottomland hardwoods, young pine plantations, and old growth pine stands. Loblolly pine is a fast growing pine extensively planted for lumber and pulpwood being widely cultivated in the southern United States. Besides various anthropogenic uses (e.g. furniture, pilings) it is also used as a windbreak and to stabilize eroded soil. The topography of the study area is characterized by gentle slopes with elevation ranging from 62 to 105 m.

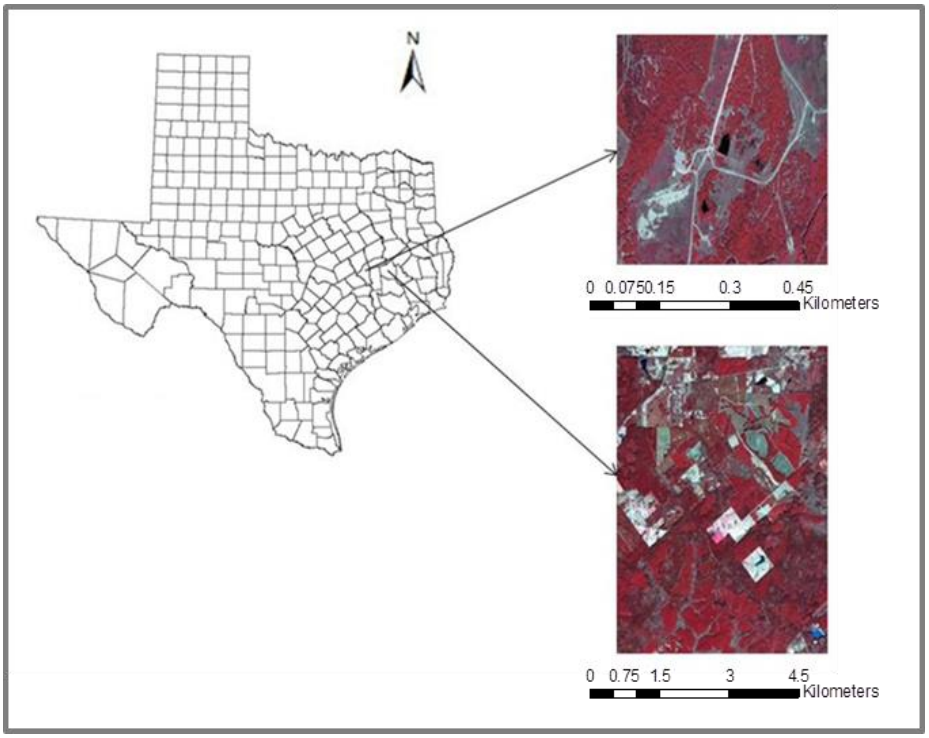

Figure 2. Study site 1: ESSM range area, located in College Station, TX and study site 2 located in Huntsville, TX shown as a false color composite of national agricultural imagery program (NAIP) image.

2.2.2 Terrestrial Laser Scanning (TLS) Data

The scans were conducted using Leica ScanStation2, a high point density 3D laser scanner (Figure 3), which emits visible green light pulses (532 nm) with a scan rate of 50,000 pulses per second. Single point accuracies of 4 mm for distance measurement and 6 mm for positional measurement from 1 to 50 m can be achieved with this scanner. The maximum field-of-view is 360º horizontal and 270º vertical. At site 1, leaf-on and leaf-off scans were conducted in November, 2010 and February, 2012 respectively (Figure 4). Site 1 consisted in a group of 21 post oak trees that were scanned from two opposite directions to avoid laser shadows as much as possible. The different algorithms

developed to retrieve DBH were first tested on the data collected at site 1. At site 2, only single scans (360° center scans) were conducted for seven plots in November 2009 and two plots in November 2012 (Figure 5).

For both sites, two stationary reference targets were used while scanning the plots, which allowed us to geo-register the scans. The position of the scanner was recorded using a differential global positioning system (GPS), and the azimuth to targets was measured using a compass. Scans for the study sites were conducted with a point density of one laser pulse within 10 cm x 10 cm at a distance of 50 m. As commonly noted in literature, multiple high-resolution scans were time consuming compared to single scan (Aschoff and Spiecker, 2004; Bienert *et al*., 2006). At study site 1, the scan time was approximately 1.5 hours, with two-direction scans conducted in 2010 and 2012. The single scan time for study site 2 was 40 min for each plot.

Figure 3. Leica ScanStation2, located over the center of a scanner setting at study site 1.

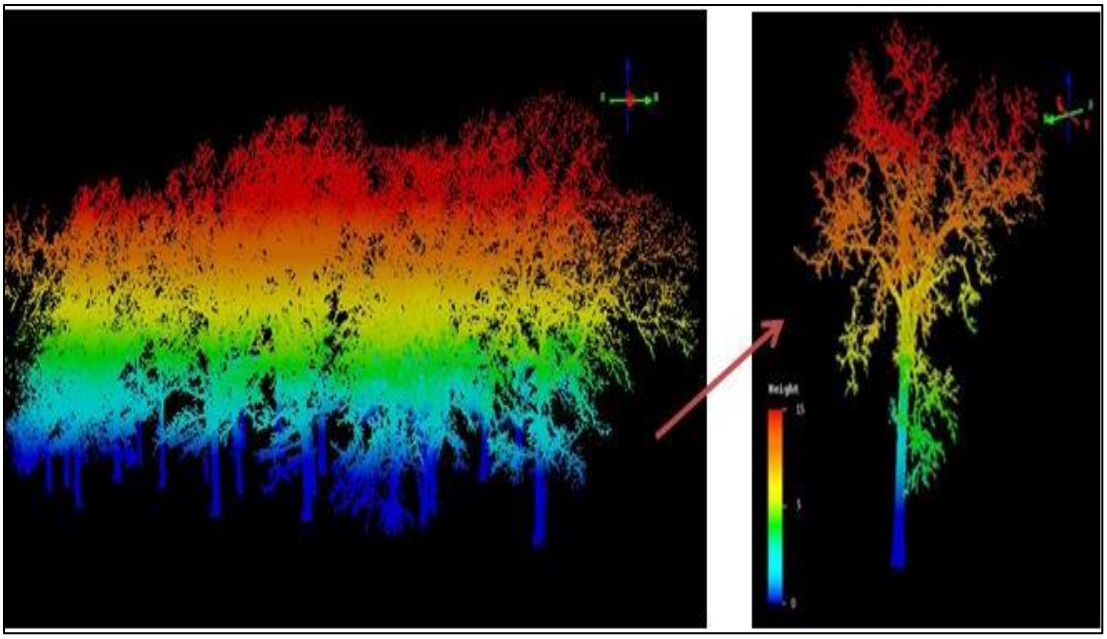

Figure 4.TLS point cloud for study site 1 highlighting an individual post oak tree. The point cloud is colored by the above ground level (AGL) heights.

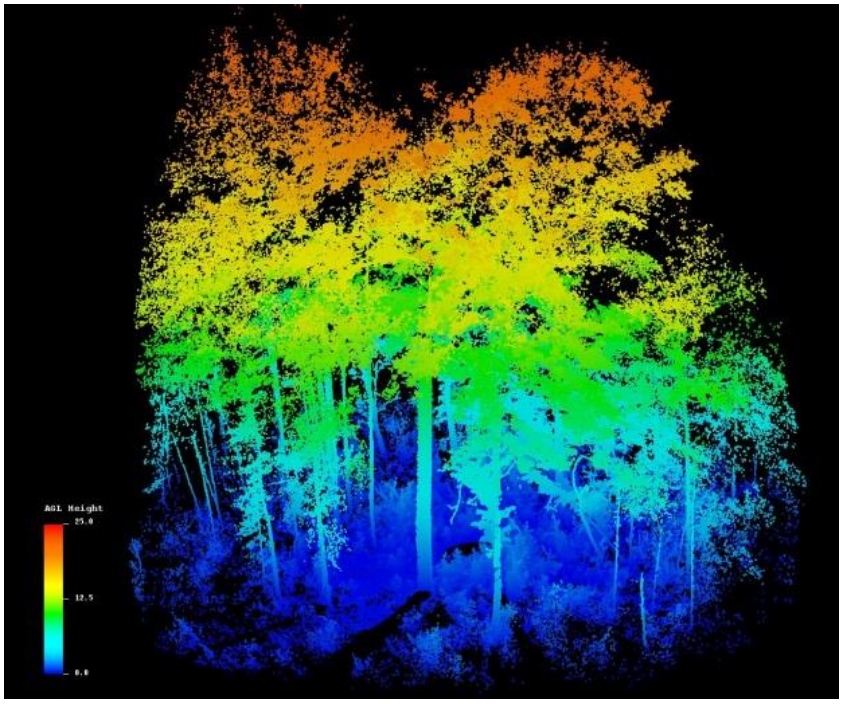

Figure 5.TLS point cloud for a (1/10th) acre circular plot at study site 2.

2.2.3 Ground Inventory Data

At site 1, field measurements (tree height, DBH, and distance and azimuth from plot center) were recorded for each tree. At site 2, tree species, height, DBH, crown width, and distance and azimuth from plot center were recorded for each tree. Crown width was calculated as the average of two values measured along the north-south and east-west directions of the crown. A laser technology Inc (LTI) TruPulse 360 laser range finder was used to find the distance and azimuth to each tree, and measure the tree height and crown width. A diameter tape was used to measure DBH to the nearest tenth of an inch. The coordinates of each plot center and positions of reference targets were recorded by point averaging using a wide area augmentation system (WAAS) enabled

Trimble global positioning system (GPS). Post-processing of GPS data included differential correction using Trimble's Pathfinder software. Ground heights derived from a digital elevation model (DEM) were assigned to the differentially corrected points.

2.2.4 TLS Data Processing

The 3D virtual point clouds obtained from the scans were unstructured data and were reconstructed by dedicated programs to provide required information such as heights (Dassot *et al*., 2011). Registration of the scans for site 1 was done in 3D point cloud processing software, Cyclone (Leica Cyclone, Version 7.1.3), wherein three common points for both the scans were selected and constraints were added. Registration was not required for site 2, since only single scans were conducted at each plot. Once registration was complete, geo-registration was performed, wherein individual scans from two different local coordinate systems were transformed into a common coordinate system. Coordinates of the scanner's position and azimuth to a stationary target were used to complete the geo-registration. While geo-registering the scans, the X and Y coordinates (easting and northing) for the scanner position were added from the GPS measurements. The Z coordinate (height) was calculated by adding the height of the scanner to the z value obtained from a 0.5 m digital elevation model (DEM) generated from airborne lidar data available for the study sites.

The point cloud was then exported to an American standard code for information interchange (ASCII) file for further processing in Quick Terrain Modeler (QTM) software (Applied Imagery, 2010). Co-registration of the scans (Figure 6) was performed using QTM software. The scans from two different years at site 2 were aligned together

to extract the same area for data processing and analysis. Since reference targets were not used while scanning site 1 in 2010 and site 2 in 2009, co-registration was used to assign a coordinate system to the unregistered TLS point cloud. Above ground level (AGL) point heights were calculated in QTM by subtracting DEM values from corresponding point elevations. All the points with heights less than 0.5 m were considered as ground returns and filtered for further analysis. This height threshold was selected to minimize the effects of low lying vegetation and rocks, and preserve the information useful to estimate different forest structural parameters. In addition, since one of the height bins for the retrieval of DBH using cylinder fitting was from 1.0-1.6 m, a height threshold of 0.5 was appropriate.

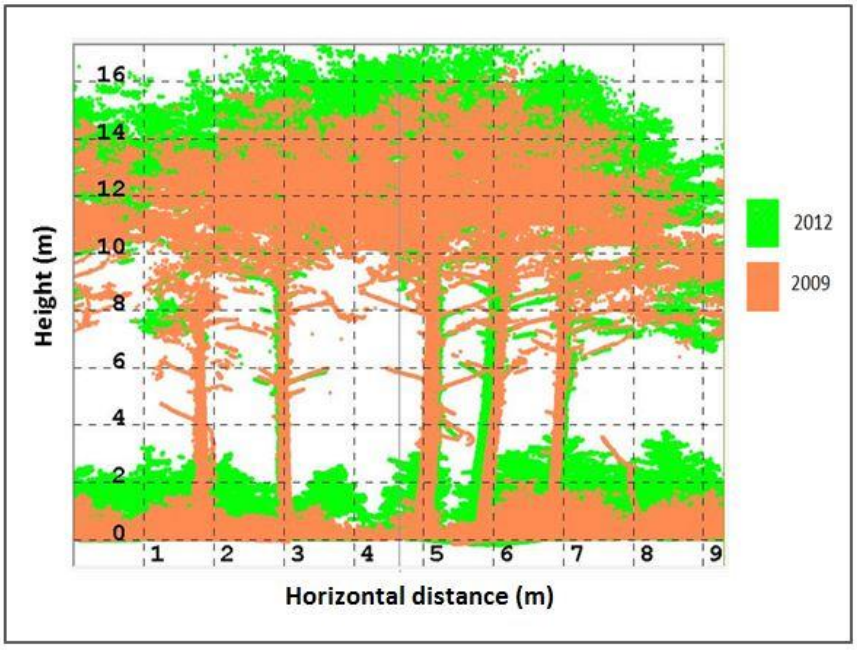

Figure 6. Co-registered TLS point cloud data from 2009 and 2012 for a plot dominated by loblolly pines at site 2.

The trees at each plot were mapped using the distance and azimuth collected during our field survey, which allowed us to validate lidar and field measurements of different forest structural parameters. A "Map Trees" tool was created using ArcObjects, which can automatically map the trees using the co-ordinates of the plot center, distance and azimuth to each tree (Figure 7). This tool minimized the field survey time since GPS coordinates for each tree need not be collected.

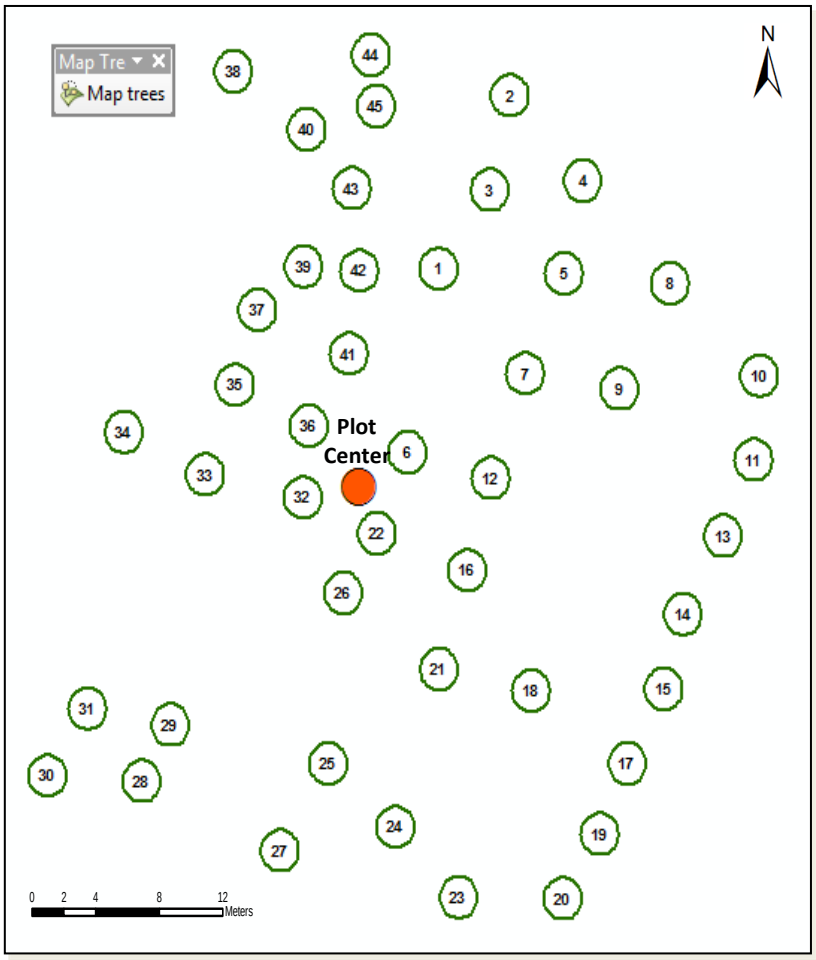

Figure 7. Stem map created using the "Map Trees" tool for a 1/10th acre plot at site 2.

0.5 m buffers were generated for each mapped tree location and were overlaid on the TLS point cloud to verify if the trees mapped using the "Map Trees" tool matched with the scanned trees (Figure 8).

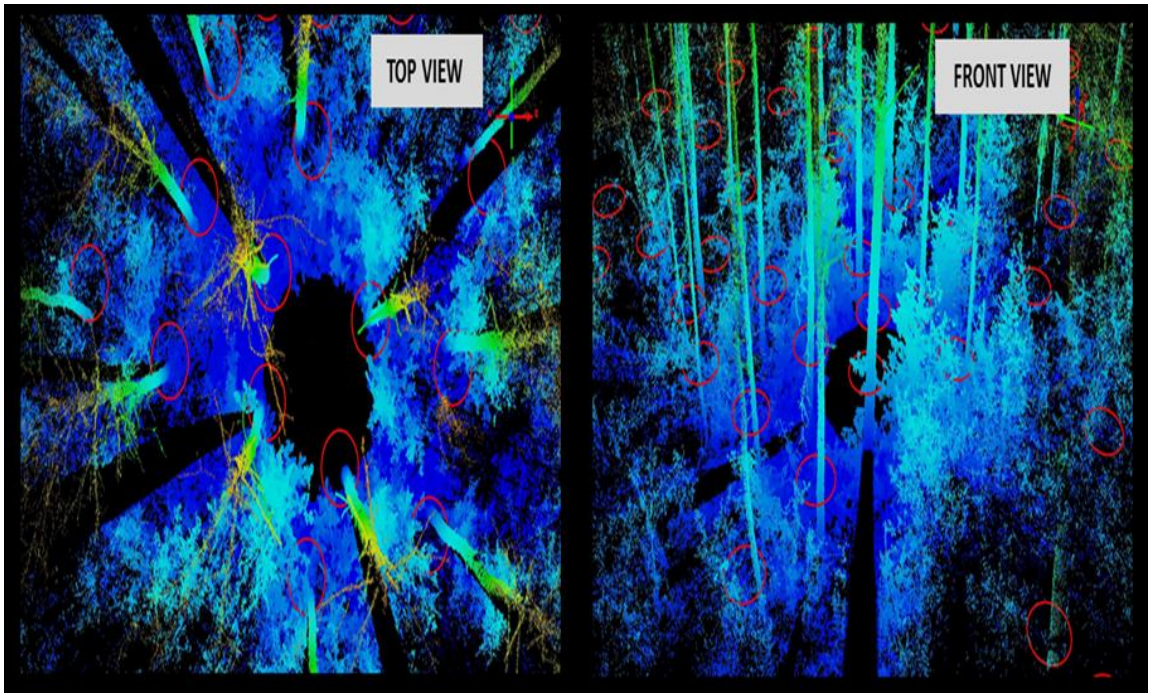

Figure 8. Mapped trees using distance and azimuth overlaid on the TLS point cloud for a 1/10th acre plot, site 2.

2.2.5 Retrieval of DBH by Cylinder Fitting

For DBH measurements, height bins of two different sizes were extracted for the plot at site 1, and three different sizes were extracted for plots at site 2 using R statistical software (version 2.13.1). Once the height bins were extracted, the point clouds were cleaned manually to remove the remaining low lying vegetation, to accurately fit

cylinders to retrieve DBH using Leica Cyclone. Figure 9 shows the height bin from 1.2-1.4 m for each of the scanned trees at site 1. The points were colored by AGL heights.

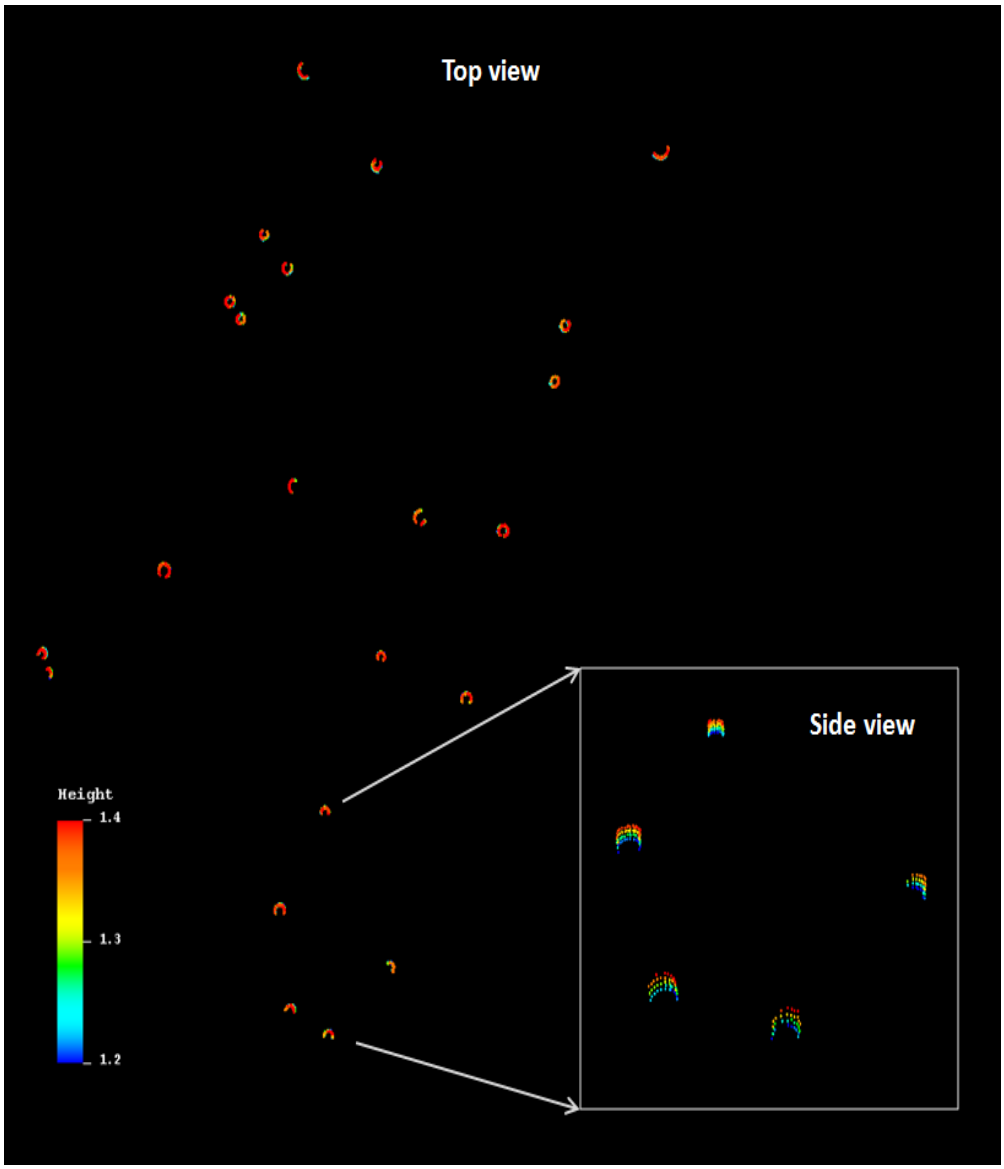

Figure 9. 1.2-1.4 m height bin for 2012 TLS point cloud at site 1.

DBH was retrieved from TLS datasets using four different methods for site 1: (a) cylinder fitting on 1.2-1.4 m height bin; (b) cylinder fitting on 1.25-1.35 m height bin; (c) calculation of average diameter between the North-South (N-S) and East-West (E-W) edges; and (d) calculation of average DBH of (a) and (c) (Figure 10). 20 cm and 10 cm height bins were used at site 1 because two-direction scans were conducted and sufficient TLS points were available in the height bins. Hence, increased size height bins were not required. DBH for trees located at site 2 were retrieved by fitting cylinders on three different height bins: (a) 1.2-1.4 m; (b) 1.1-1.5 m; and (c) 1.0-1.6 m. Since only single scans were conducted at site 2, increased size height bins of 20 cm, 40 cm, and 60 cm were required to retrieve DBH. Points which deviated most from a fitted cylinder were considered noise and removed for DBH measurements. The best cylinder fitting method to estimate DBH was also investigated. Further, this study also addressed the influences of tree distance from the scanner, number of points to fit the cylinder, number of scans (single vs. two-direction scans), and height bin size on DBH estimation accuracy.

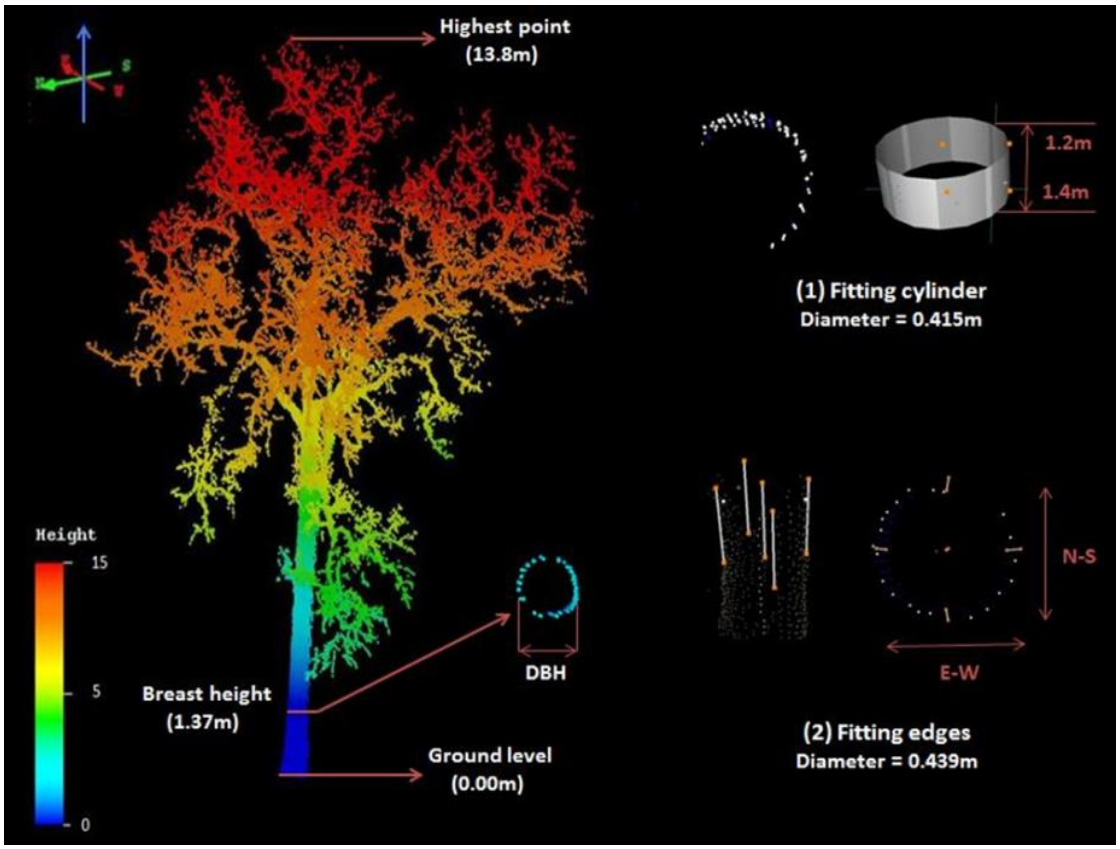

Figure 10. DBH retrieval methods from TLS data.

2.2.6 Extraction of Individual Trees from TLS Point Cloud

Individual trees were extracted at each plot to retrieve tree heights and crown widths. The first step was to extract point clouds for individual trees by isolating points using a cylinder with diameter equal to an expected crown width for each tree. In this study, a relationship between field measured crown widths and DBH was established from field surveys conducted in 2004. Figure 11 shows the regression results of field measured crown widths and DBH for 200 loblolly pine trees in Huntsville, East Texas. A high R-squared value of 0.9260 was obtained. The coefficients to predict crown

widths were obtained separately for different tree species such as loblolly pines, sweet gum (*Liquidambar*), and oaks (*Quercus*) (Table 2).

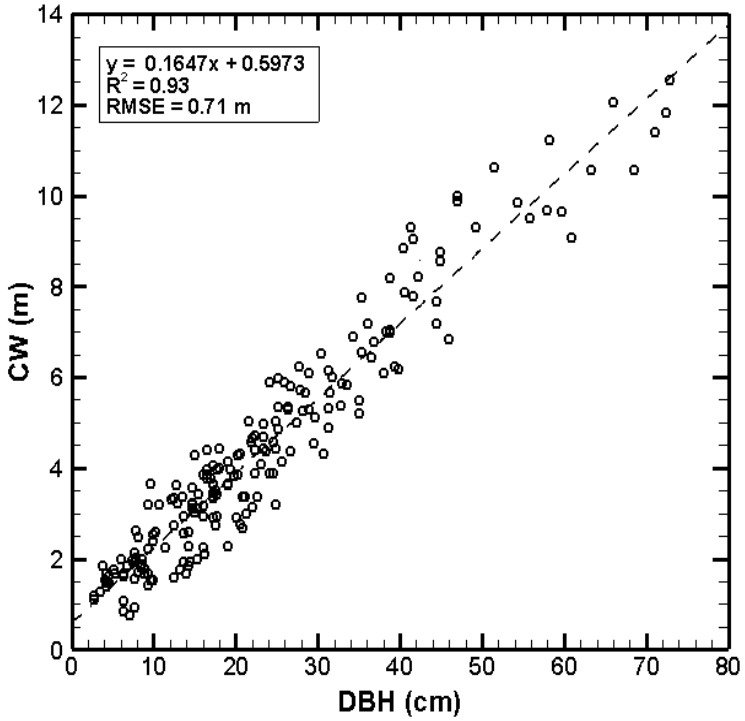

Figure 11. Scatter plot of simple linear regression result for field measured crown width and field measured DBH

Table 2. Regression results of field measured crown width (CW) and DBH.

Species	Number of trees	Equation	R^2	RMSE (m)
Loblolly pine	200	CW = 0.5973 + 0.1647 * DBH	0.93	0.71
Sweet gum	80	CW = 1.2946 + 0.1950 * DBH	0.77	0.67
Oak	100	CW = 0.7927 + 0.2635 * DBH	0.81	1.26

The crown widths were used as the distance variable in the buffer tool in Arcmap, and buffers were created for each tree mapped using the previously mentioned map trees tool. The individual trees were extracted using vertical cut cylinders in QTM obtained using the crown width buffers (Figure 12). After extracting the individual trees from lidar point cloud, visual inspection was done to manually remove the points from adjacent crowns or stems if present (Hopkinson *et al*., 2004).

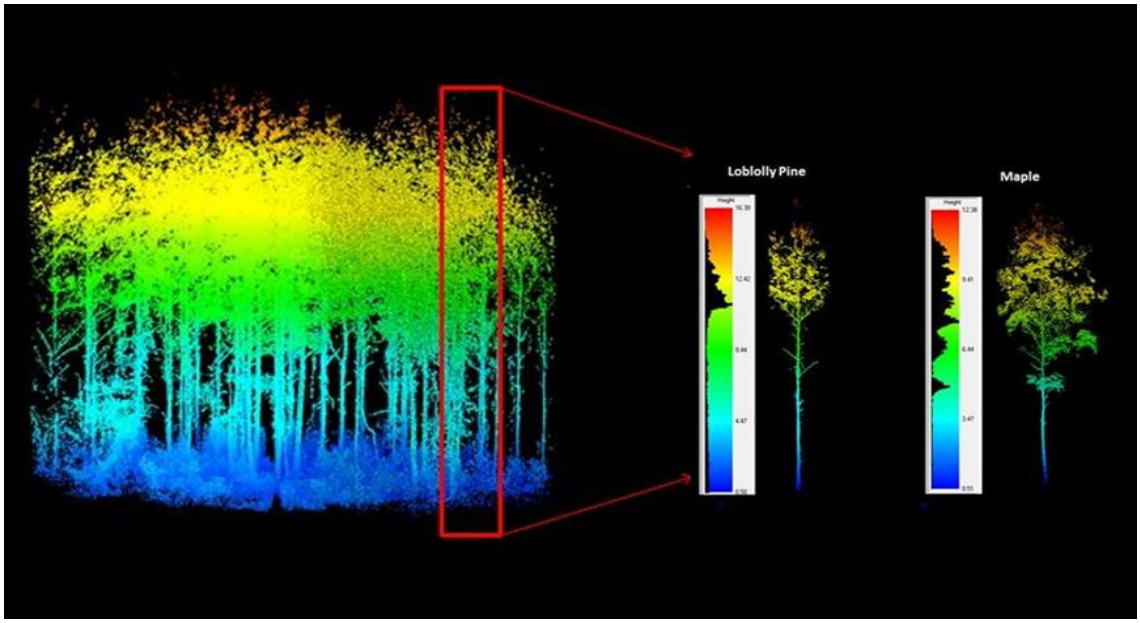

Figure 12. Extraction of individual trees using crown widths predicted from TLS derived DBH.

2.2.7 Retrieval of Tree Height and Crown Width

Since crown widths were not measured at site 1, individual tree heights were calculated as the highest point in cut cylinders of varying radii (Maas *et al*., 2008).

Range rings or buffers were created in QTM with different radii such as 0.5 m, 0.8 m, and 1 m depending on the DBH of the trees (Figure 13). Range rings of 0.5 m radii were created for trees with smaller DBH values.

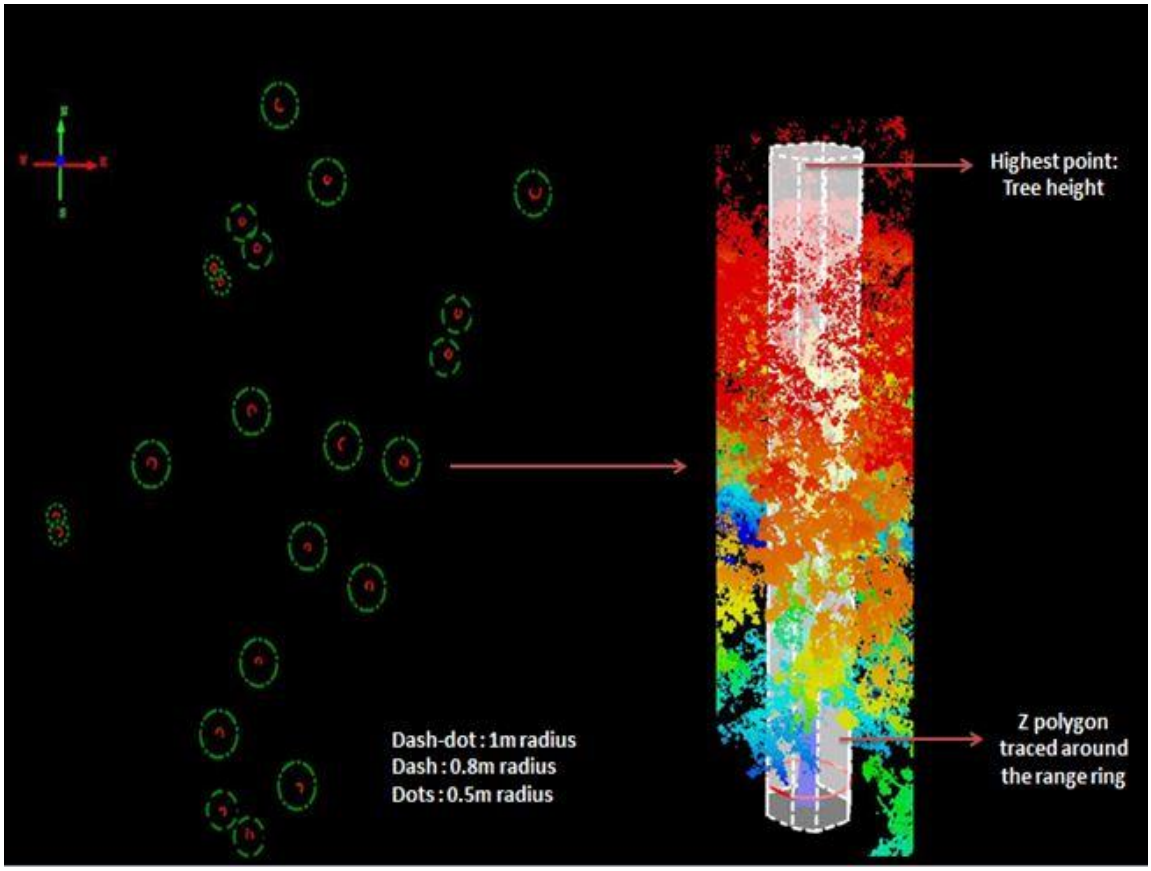

Figure 13. Retrieval of tree heights at site 1 using cut cylinders.

A different approach was implemented to compute tree heights at site 2. FUSION/LDV (Lidar Data Viewer) software is a powerful open source lidar data analysis and visualization system developed by the USDA Forest Service, which also

includes a collection of task-specific command line programs (McGaughey, 2007). The extracted individual trees were input to CloudMetrics algorithm in command line utility. Tree heights were automatically computed by the algorithm in addition to several other statistical parameters.

Crown widths were obtained using FUSION and LDV. Measurement cylinders were set over each tree (Figure 14), and the diameter was adjusted to compute the crown width. For trees with nearly circular crowns, the minimum and maximum crown widths were the same. For trees with irregular crowns, the aspect ratio of the measurement marker was adjusted to closely match the shape of the crown. Then, the average of minimum and maximum crown widths, which correspond to the minor and major axes of the measurement disk, was calculated as the crown width of the tree.

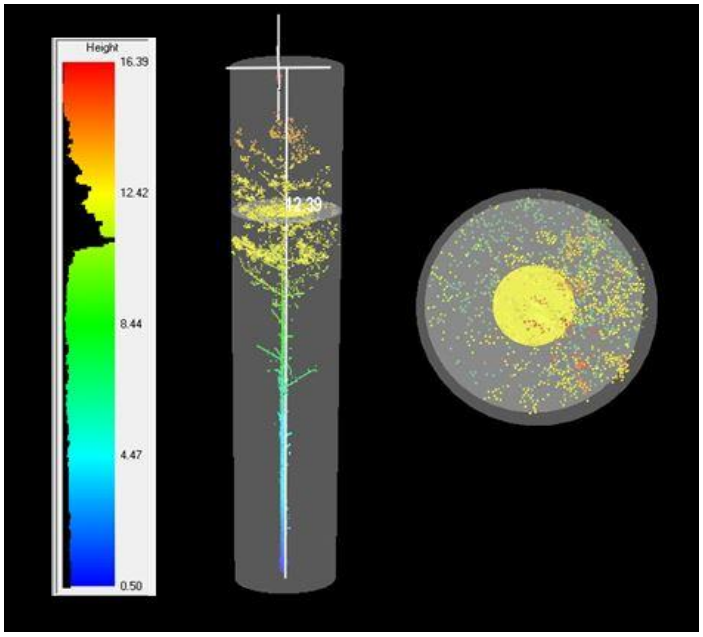

Figure 14. Measurement disk fitted on a tree to compute crown width.

2.3 Results and Discussion

2.3.1 DBH Measurement by Cylinder Fitting

For TLS derived DBH at site 1, validation against field measured DBH indicated a high R-squared value of 0.95 for cylinder fitting using 1.2-1.4 m height bin.
The R-squared values for DBH retrieval using TLS datasets for methods (b), (c), and (d) were 0.91, 0.92, and 0.94 respectively. Since two-direction scans were conducted at site 1, a 20 cm height bin was sufficient to derive DBH from the point cloud. The problem of sparse laser points due to shadowing was not experienced at this site.

The purpose of fitting cylinders with three different height bins at site 2 is presented in figures 15 and 16. Two trees at distances 1.22 m (tree 1) and 10.51 m (tree 2) from the plot center were extracted from the TLS point cloud data. When three height bins were generated for both trees, it was seen that tree 1 had sufficient number of laser points in all the height bins to fit a cylinder due to no occlusion caused by other trees, whereas tree 2 had very few laser points in the 1.2-1.4 m height bin due to shadowing from other trees. When the bin size for cylinder fitting was increased from 20 cm to 40 cm and 60 cm for tree 2, TLS derived DBH were 20.9 cm and 21.5 cm respectively, which are close to the field measured DBH (22.3 cm). Since previous studies have discussed that DBH cannot be reliably measured with sparse laser points (Bienert *et al*., 2006; Brolly and Kiraly, 2009; Huang *et al*., 2009), estimates of DBH must be retrieved using different height bins.

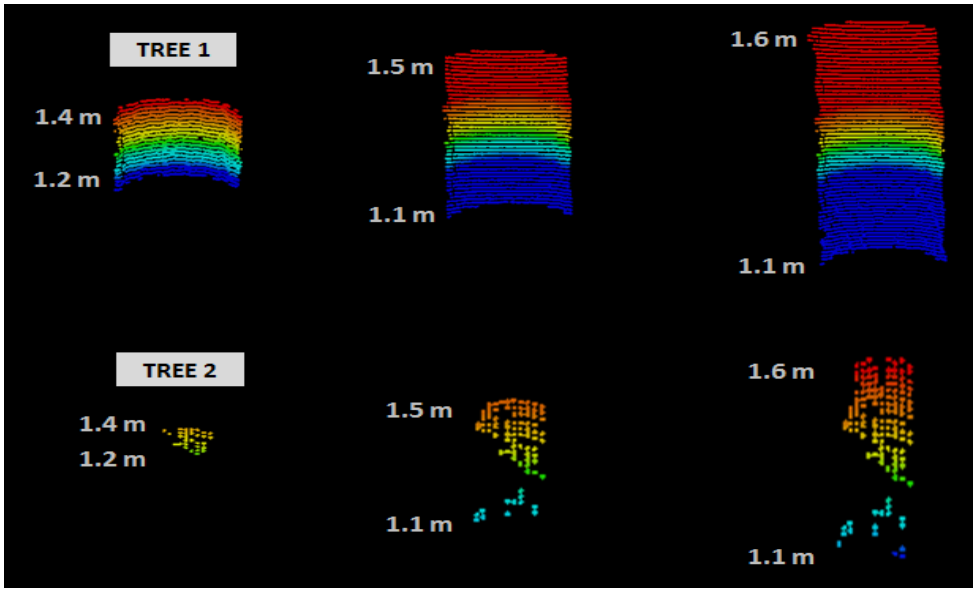

Figure 15. Three height bins of two loblolly pines at site 2 extracted for cylinder fitting.

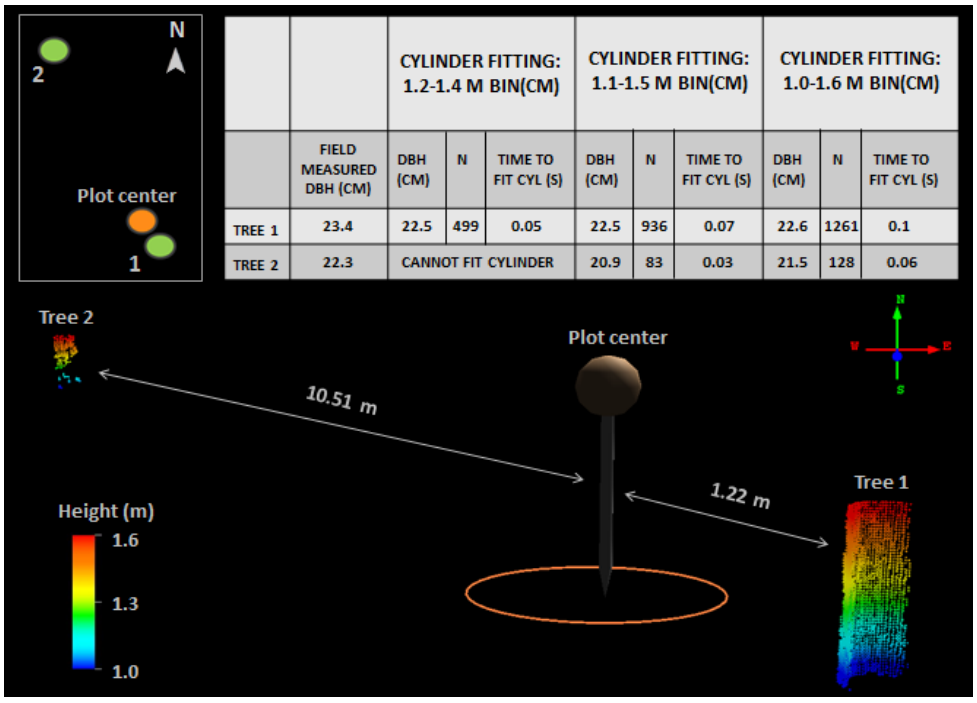

		CYLINDER FITTING: 1.2-1.4 M BIN(CM)			CYLINDER FITTING: 1.1-1.5 M BIN(CM)			CYLINDER FITTING: 1.0-1.6 M BIN(CM)		
	FIELD MEASURED DBH (CM)	DBH (CM)	N	TIME TO FIT CYL (S)	DBH (CM)	N	TIME TO FIT CYL (S)	DBH (CM)	N	TIME TO FIT CYL (S)
TREE 1	23.4	22.5	499	0.05	22.5	936	0.07	22.6	1261	0.1
TREE 2	22.3	CANNOT FIT CYLINDER			20.9	83	0.03	21.5	128	0.06

Figure 16. Cylinder fitting results on 1.2-1.4 m height bin for tree 1 and tree 2.

Overlay plots created for 2009 and 2012 TLS derived DBH from 1.0-1.6 m height bin for a plot at site 2 (Figure 17) illustrated the change in DBH for all the trees.

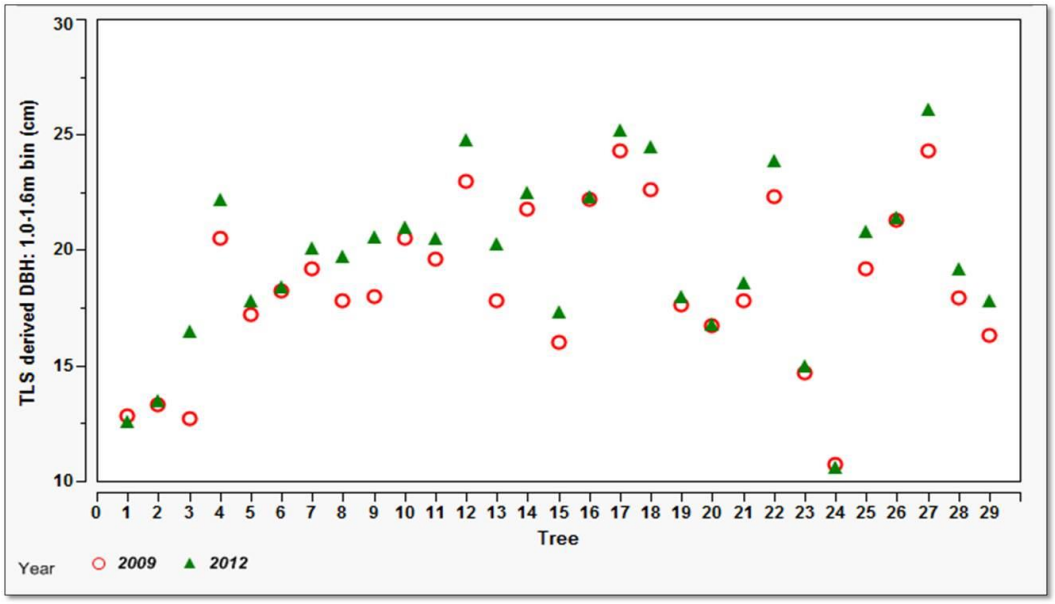

Figure 17. Overlay plot for TLS derived DBH using 1.0-1.6 height bin.

Table 3 shows the regression results of field measured DBH and TLS derived DBH using three height bins for site 2. Though the R-squared values for all three methods were high, the number of trees detected using 1.2-1.4 m height bin was low compared to the other two methods. Only 83% of the trees were detected and available for cylinder fitting to retrieve DBH (Figure 18). For a few trees, the number of points within the 1.2-1.4 m height bin was insufficient to fit a cylinder. This might be due to the shadowing from other stems or heavy understory. The RMSE value was also high compared to the other two height bins (Table 3), which indicated that cylinder fitting on

1.2-1.4 m height bin would not be the best method to retrieve DBH from single scans. Cylinder fitting on 1.1-1.5 m and 1.0-1.6 m height bins provided similar R-squared values and RMSE (RMSE values of 1.83 and 1.85 cm respectively and R-squared value of 0.97). Compared to cylinder fitting on 1.2-1.4 m height bin, the RMSE decreased by approximately 0.29 cm and the stem detection rate increased by approximately 17%. These results show that cylinder fitting on an increased height bin size provide promising results for the retrieval of DBH from single scan TLS datasets.

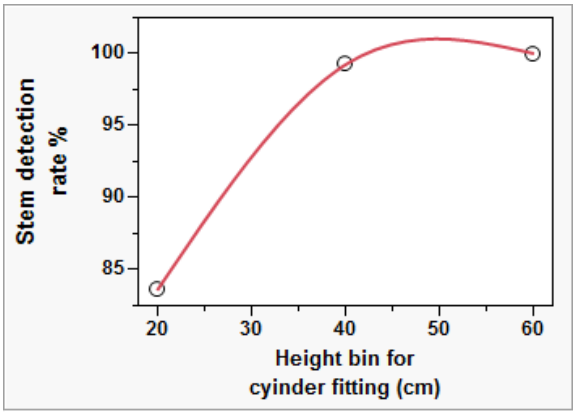

Figure 18. Stem detection rate based on the three height bins used for cylinder fitting.

Table 3. Results of field measured DBH and TLS derived DBH by cylinder fitting using three different height bins.

Height bin (m)	Number of trees fitted with cylinders	R^2	RMSE (cm)
1.2-1.4	122	0.96	2.13
1.1-1.5	145	0.97	1.83
1.0-1.6	146	0.97	1.85

The accuracy of TLS derived DBH was influenced by several other factors such as ranging method, number of scans, and DBH extraction method. The result illustrated in figure 19 concurred with the findings of Pueschel et al. (2013), who reported that range does not influence the accuracy of DBH estimation; however for lower scan resolutions and longer ranges, DBH estimation accuracies might decrease due to reduced point density. Figure 20 shows the DBH residuals as a function of the number of points to fit 1.0-1.6 m cylinder. DBH residual is the difference between the field measured DBH and TLS estimated DBH. Though a strong relationship was not seen, the residuals were large for a few stems that had lower number of points to fit the cylinder.

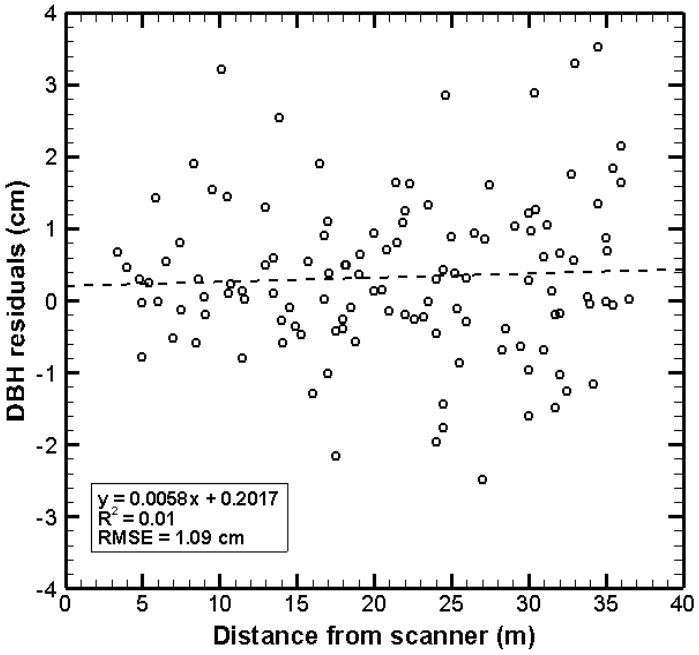

Figure 19. DBH residuals as a function of distance from scanner.

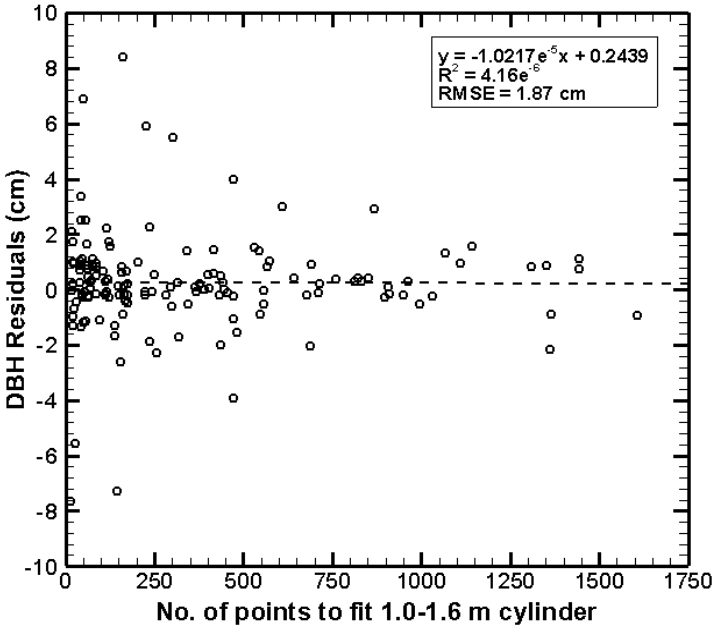

Figure 20. DBH residuals as a function of number of points to fit the cylinder.

The minimum, maximum, and average number of points to fit the cylinders using 1.2-1.4 m, 1.1-1.5 m, and 1.0-1.6 m height bins at site 2 is summarized in table 4. Since sufficient laser points were available for cylinder fitting using two-direction scans at site 1, the number of points used for cylinder fitting was not recorded.

Table 4. Descriptive statistics for cylinder fitting on single scan data.

	Number of points to fit the cylinder		
Cylinder fitting height bin (m)	Min	Mean	Max
1.2-1.4	7	126	544
1.1-1.5	10	245	1105
1.0-1.6	16	359	1608

Considering the number of scans and height bin size, a smaller height bin (1.2-1.4 m) was sufficient to estimate DBH from two-direction scans. However, for single scans, cylinder fitting using increased height bin size provided promising results. The use of merged scans for DBH measurements is advantageous due to multi-angular coverage (Thies and Spiecker, 2004; Bienert *et al*., 2006); potentially increasing stem detection rates, but is time consuming. Pueschel et al. (2013) found that DBH determined from two-direction scans have lower RMSE's ranging from 0.66-1.21 cm compared to single scan data with RMSE's ranging from 1.39-2.43 cm. The results of this study indicated that RMSE for the best DBH extraction method was 0.74 cm for two-direction scans 1.83 cm for single scan data.

2.3.2 Retrieval of Tree Height and Crown Width

Van Leeuwen and Nieuwenhuis (2010) reviewed several studies and discussed the accuracy with which different forest inventory parameters can be retrieved using lidar. Generally, field measured tree heights are underestimated compared to lidar derived heights. As reported in the literature, R-squared values range from 0.75 to 0.98 for individual tree heights derived from airborne lidar. For TLS derived tree heights, RMSE values range from 1.4-4.4 m. In this study, for site 1, the R-squared value was 0.66 when TLS derived heights using vertical cut cylinders were regressed against field measured heights. The lower R-squared value could be largely attributed to the time lag between the field measured tree heights collected in August, 2012 and acquisition of TLS data in March, 2012. TLS derived heights underestimated field measured heights by an average of 0.6 m. Another possible reason for the unexplained height variance is that

the method for tree height estimation at site 1 could result in underestimation of field measured heights for irregular crowns, because the highest point might not always be found at the center of the tree crown.

The method used to retrieve tree heights from TLS data in site 2 was more automated and provided promising results. The R-squared value was 0.92 and RMSE was 1.51 m when field measured heights were regressed against TLS derived heights for 85 trees (Figure 21). The results agreed with the findings of Hopkinson et al. (2004) and Williams et al. (1994) that tree height measurements are less accurate in hardwood stands compared to softwood stands. It might also be expected that as the heights increase, tree height estimation errors will also increase since the laser pulses might not be able to penetrate to the tree tops completely (Van Der Zande *et al*., 2006). However, for site 2, heights had no influence on the tree height estimation, and it was observed that field measured heights were overestimated by an average of 0.30 m compared to TLS derived heights. This might be due to the misidentification of true tree tops during field survey as some plots had dense overstory. Field measured heights were underestimated in cases where shadowing was prevalent, which occluded the tree tops.

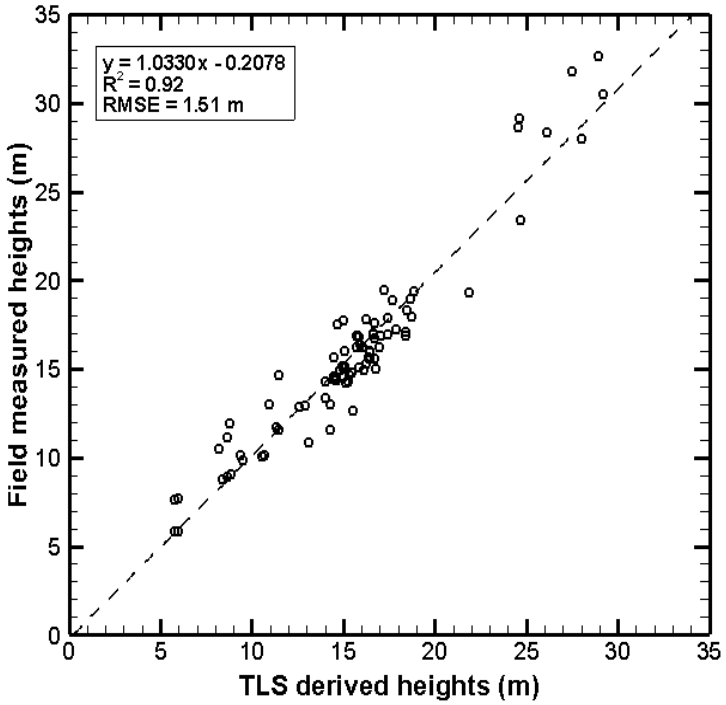

Figure 21. Scatterplot of regression result for field and TLS derived tree heights.

TLS derived crown widths for site 2 were validated using field measured crown widths for 67 trees (Figure 22). The R-squared value was 0.84 and RMSE was 1.08 m. This was significantly high compared to other studies, which derived crown widths from airborne lidar data (e.g. Naesset and Oakland, 2002). Field measured crown widths were underestimated by an average of 0.85 m, which was expected because field measurements provided overlapping crown widths, since the entire span of the crown was measured in the field, while TLS measurements provided only non-overlapping crown widths (Popescu *et al*., 2003) (Figure 23).

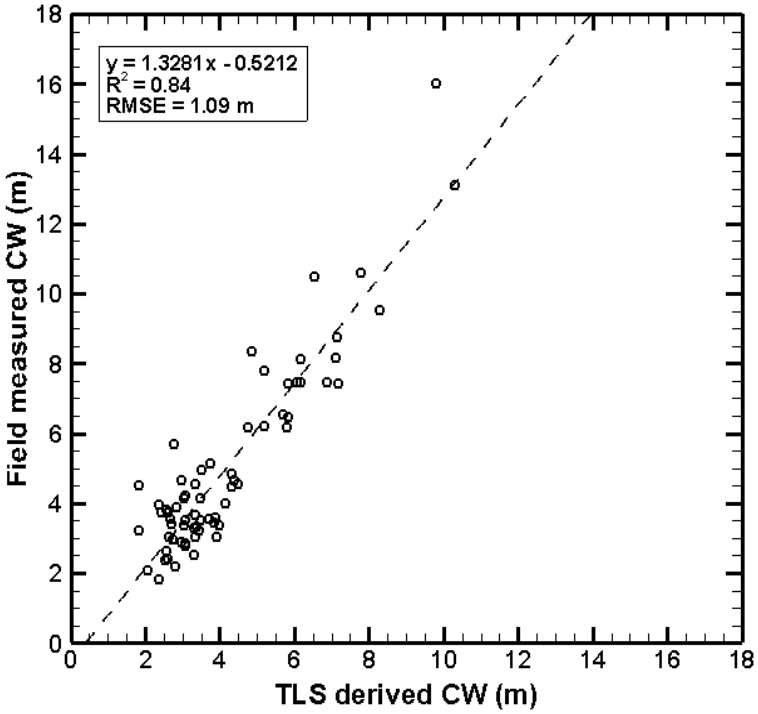

Figure 22. Scatterplot of regression result for field measured crown width and TLS derived crown width.

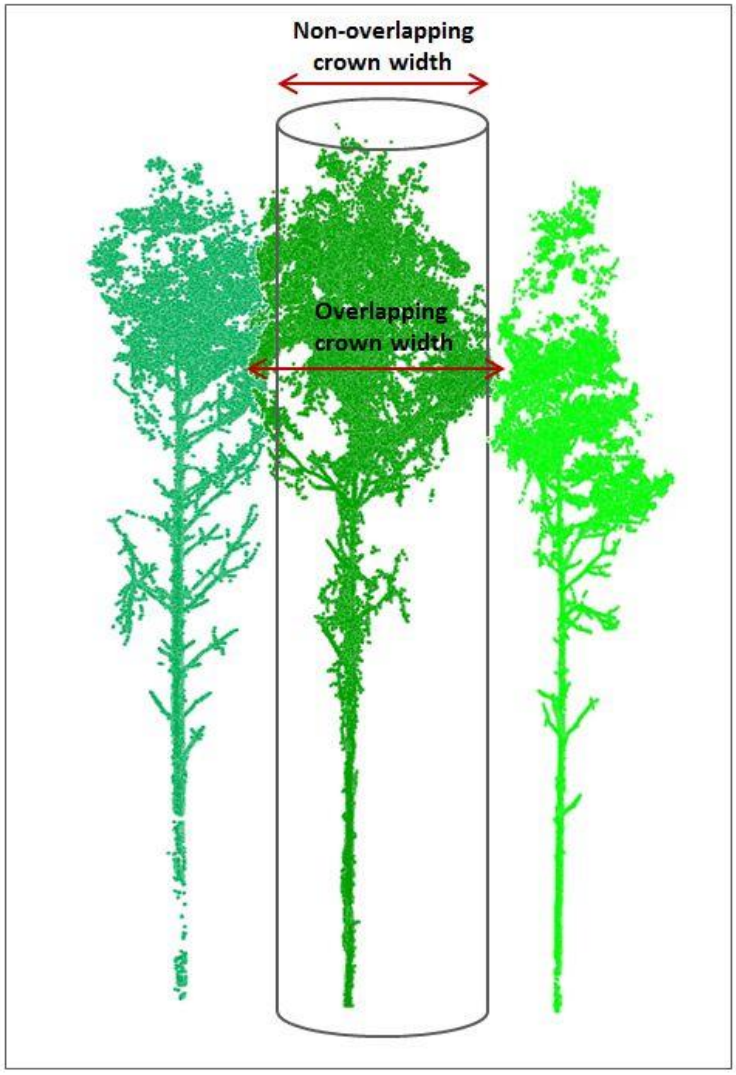

Figure 23. Non-overlapping crown width obtained from TLS measurements and overlapping crown width obtained from field measurements.

A positive correlation between the crown width residuals and crown widths (Figure 24) was observed. Crown width residuals are calculated as the difference between field measured crown widths and TLS derived crown widths. As crown width increases, the interaction with neighbouring trees also increases, which further increases

the variance between field measured and TLS derived crown widths. Field measured crown widths were also overestimated when compared to crown widths derived from TLS datasets in a few cases, where the complete extraction of an individual tree was not possible due to increased interference from adjacent crowns.

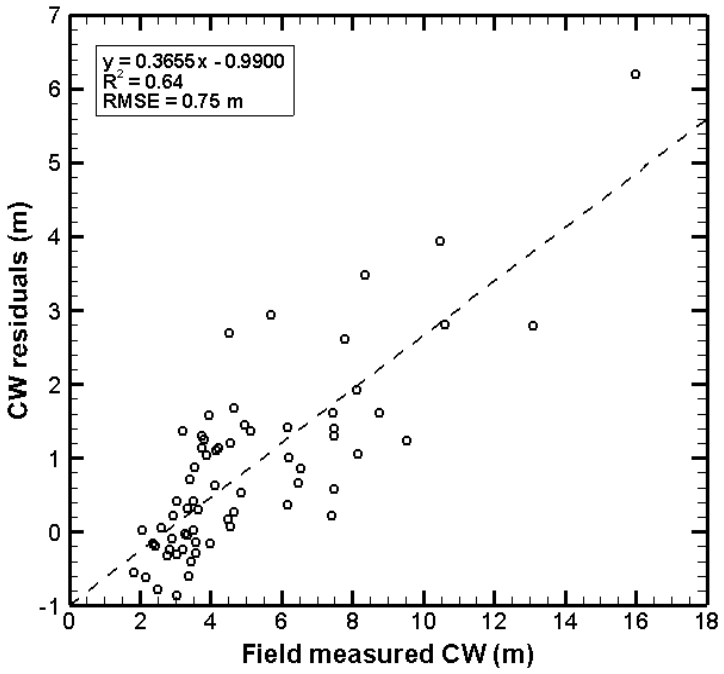

Figure 24. Crown width residuals as a function of crown width.

2.3.3 Influence of Tree Shadowing on the Accuracy of Deriving Tree Measurements

Histograms were generated for a post oak tree at site 1 (Figure 25). It can be clearly seen that for the post oak tree at site 1, an increased number of laser hits was observed for leaf-on scans at lower heights and fewer laser hits were present on the upper part of the tree due to the occlusion caused by other trees, while the number of

laser hits in the leaf-off scans were greater for the upper part of the tree due to less occlusion. Tree tops could be missed due to shadowing while conducting leaf-on scans, leading to the underestimation of field measured tree heights.

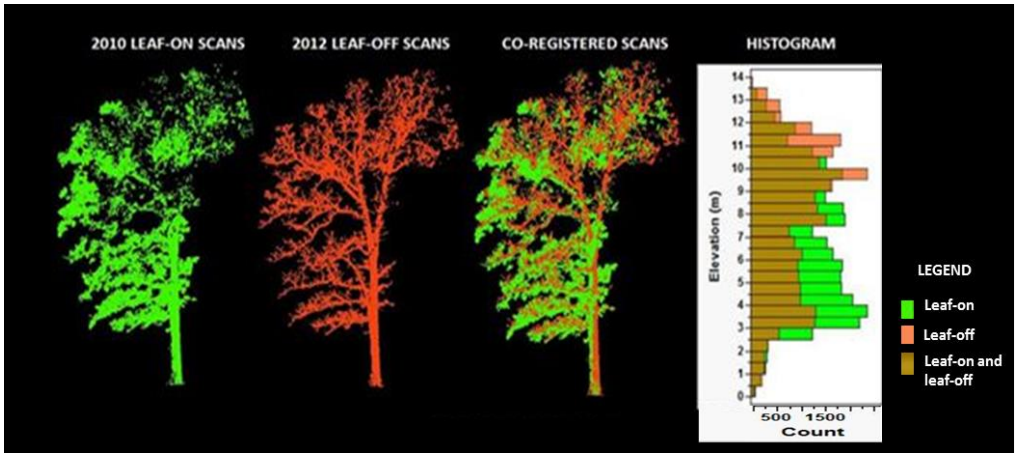

Figure 25. Histogram overlay analysis for a post oak tree at site 1.

Figure 26 depicts the influence of tree shadowing, which results in the reduction of laser pulse penetration in a plot subset at site 2. The highlighted tree 11 was shadowed by tree 12, which prevented the laser pulses from the scanner set at the plot center to fully reach the tree crown. Hence, TLS derived tree height underestimated field measured tree height by 4.47 m. The figure also shows another highlighted tree 8, which is at a distance of 10.42 m from the scanner and is also obstructed by tree 7. The heavy understory and tree 7 have minimized the penetration of laser pulses to tree 8. This led to the underestimation of field measured tree height by 4.28 m. As the tree density and branching increases, the quality of information obtained from TLS decreases. Two-

direction scans can reduce the errors due to occlusion, but they are time consuming (Van Leeuwen and Nieuwenhuis, 2010). Thus, it is very important to understand the laser pulse penetration through the canopy to reduce the uncertainties in the estimation of different forest structural parameters.

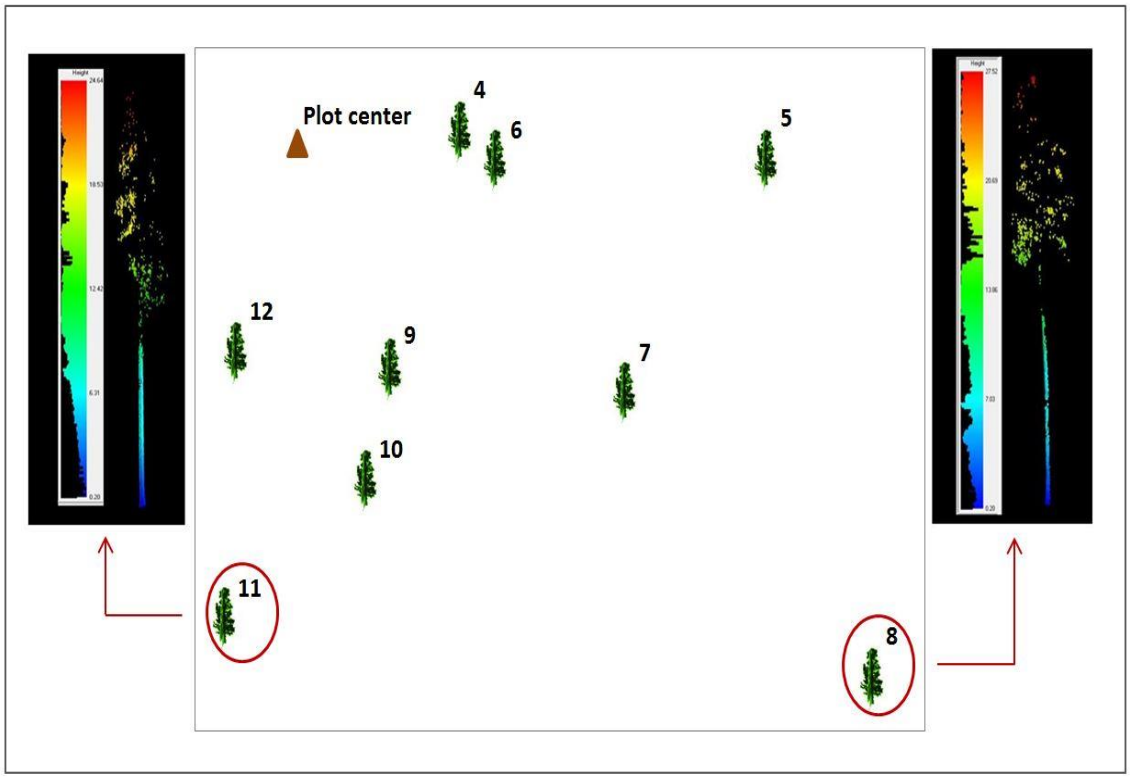

Figure 26. Reduction of the laser pulse penetration due to tree shadowing.

2.4 Conclusions

The efficacy of terrestrial lidar in retrieving different forest structural parameters rapidly and accurately at an individual tree level using novel methods was clearly demonstrated in this study. Some of the new methods implemented in this study were cylinder fitting on three different height bins to retrieve DBH, tree mapping using an automatic tool developed in ArcObjects, extracting individual trees from TLS point clouds to retrieve tree height and crown width, and investigating the influence of the number of scans on DBH estimation accuracy. For site 1, due to two-direction scans and adequate laser point densities in the 1.2-1.4 m height bin, increased height bin size for cylinder fitting may not be required to retrieve DBH. For the circular plots at site 2, cylinder fitting with increased height bin size provided improved accuracies for DBH estimates from single scan TLS data. A high R-squared value of 0.97 and RMSE of 1.85 cm were obtained when DBH retrieved by cylinder fitting on 1.0-1.6 m height bin were validated against field measured DBH. For site 1, the mean height decreased from 2010 to 2012 due to leaf-on and leaf-off scans respectively, while individual tree level heights increased from 2010 to 2012. For site 2, as leaf-on scans were conducted for both the years, tree height increased from 2009 to 2012. The R-squared value was 0.84 when field measured crown widths were validated against TLS derived crown widths. Underestimation of field measured crown widths were observed in this study, because overlapping and non-overlapping crown widths were obtained from field measurements and TLS data respectively.

This study also discussed the influence of number of scans, distance from scanner, cylinder fitting height bin size on the estimation of various parameters. TLS derived measurements underestimated field measurements when the laser pulses had not penetrated completely to the tree crowns due to canopy shadowing. Though an increased amount detail is obtained from two-direction scans, it is time consuming in terms of data collection and processing (Aschoff and Spiecker, 2004; Bienert *et al*., 2006; Dassot *et al*., 2011). Multiple scans should be conducted or correction factors should be applied to reduce the errors in estimation of forest structural parameters. The various metrics derived from TLS point cloud will be useful for inventory and time series analysis. Future work could investigate the potential of integrating spatially coincident airborne lidar data and terrestrial lidar data to provide an enhanced characterization of the overstory and understory.

CHAPTER III

STUDYING TREE LEVEL GROWTH AND BIOMASS CHANGE USING MULTI-TEMPORAL TERRESTRIAL LASER SCANNING DATASETS

3.1 Introduction

Accurate measures of forest structural parameters and the monitoring of their changes through time are essential to forest inventory and growth models, managing wildfires, modeling of carbon cycle, and forest management systems (Næsset *et al*., 2004). Most extant methods, which include indirect and direct measurement techniques, are limited in their capability to acquire accurate, spatially explicit measurements of forest three-dimensional structural parameters. The accuracy of these measurements can be improved using lidar (light detection and ranging) (Kussner and Mosandl, 2000; Henning and Radtke, 2006).

Lidar, which is an active sensor, emits a series of laser pulses, and measures the distance to targets based on the speed of light and travel time of the laser pulses to and from a system (Lefsky *et al*., 2002a). Unlike passive optical remote sensing, lidar remote sensing provides detailed information on both horizontal and vertical distribution of vegetation in forests (Lim *et al*., 2003). Applications of lidar remote sensing such as measurement of the structure and function of vegetation canopies and estimation of tree height, crown width, basal area, stem volume, and aboveground biomass (AGB) are elaborated in various studies (Lefsky *et al*., 2002b; Chen *et al*., 2007; Popescu and Zhao, 2008; Falkowski *et al*., 2009). Non-destructive measurements of AGB can be done using

airborne lidar with a higher accuracy compared to AGB measurements obtained through other remote sensing techniques (Lefsky *et al*., 2002a; Bortolot and Wynne, 2005; Popescu, 2007; Hudak *et al*., 2012). Nevertheless, tree height estimates with small footprint discrete return airborne lidar tend to slightly underestimate manual measurements done in the field, as the laser pulses are not always reflected from tree tops. Airborne lidar may not capture the complete vertical distribution of the canopy (Lim *et al*., 2003). Terrestrial laser scanning (TLS) fills the gap between tree scale manual measurements and large scale airborne lidar measurements by providing a wealth of precise information on various forest structural parameters (Maas *et al*., 2008; Dassot *et al*., 2011) and a digital record of the three dimensional structure of forests at a given time. Hence, to obtain accurate understory information and detailed canopy vertical structure depiction, TLS can produce better results when compared to airborne lidar and field measurements (Loudermilk *et al*., 2009).

The use of terrestrial or ground-based laser scanners for forest management planning and mapping vegetation properties has grown dramatically in the last decade (Moskal *et al*., 2009; Moskal and Zheng, 2012; Kankare *et al*., 2013). Terrestrial laser scanners have a high potential to acquire three-dimensional data of standing trees accurately and rapidly through non-destructive methods, which has resulted in the multiple use of this technology in studying forest environments (Lovell *et al*., 2003; Dassot *et al*., 2011). Several studies have shown that TLS is a promising technology in providing objective measures of tree height, diameter at breast height (DBH), stem density, canopy cover, and AGB (Bienert *et al*., 2006; Hopkinson *et al*., 2008; Maas *et*

al., 2008; Kankare *et al*., 2013). Evans et al. (2006) addressed the use of lidar for forest assessments and proposed two significant domains in which lidar could be a major contributor: tree growth and yield modelling at individual tree level for pine plantations using multi-temporal lidar data, and implementation of retrieved individual tree measurements from lidar data in immersive visualization environments for the assessment of forest stands.

AGB is defined as all the living biomass above the soil that includes stem, stump, branches, bark, seeds, and foliage; it is associated with important components such as tree health, forest regeneration, and energy conversion (Jenkins *et al*., 2003). It is a crucial ecological variable, which has to be accurately estimated to reduce the uncertainties in the estimates of forest carbon budget and understand potential changes of the climate system. Further, half of the dry biomass is considered to account for carbon, which is of great scientific interest to understand the carbon cycle (Houghton *et al*., 2009; Lin *et al*., 2010; Zolkos *et al*., 2013). Næsset et al. (2011) developed non-linear biomass models using airborne lidar derived height metrics and canopy density. The authors performed a stepwise forward selection procedure to select the best set of independent variables to estimate biomass. They observed that the estimated biomass was not statistically different from field measured biomass for lidar based models. Yao et al. (2011) used a ground-based, scanning near-infrared full waveform lidar and retrieved tree diameters and stem count density to determine aboveground standing biomass. They obtained a coefficient of determination of 0.85 between the lidar derived and field measured biomass. Lefsky et al. (2002b) developed a single equation to

estimate AGB from lidar derived canopy structure in three distinct study sites that explained 84% of the variance. Zolkos et al. (2013) combined and contrasted results from different studies on the estimation of AGB from lidar remote sensing and found that AGB estimated from remote sensing models were closely related to field measured AGB if the residual standard error was less than or equal to 20 Mg ha^{-1}. They also discussed that significantly better results for the estimation of AGB were obtained using airborne lidar data compared to radar or optical data. However, very little research has been done in estimating AGB at individual tree level with TLS data, which could be used in the detailed evaluation of silvicultural techniques (Kankare *et al*., 2013).

Lidar is also a promising technology to study growth and derive forest parameters (Hudak *et al*., 2009). Few studies have investigated forest succession using lidar to predict long-term carbon sequestration (Falkowski *et al*., 2009; Hudak *et al*., 2012). Successful modeling of change in airborne lidar estimated biomass has been done using three different approaches: (1) computing the change in biomass by subtracting the estimated biomass between two different years; (2) modeling of biomass change by a system of models; and (3) direct modeling of biomass change (Bollandsås *et al*., 2013). Hopkinson et al. (2008) assessed the plot level mean tree height growth for homogenous red pine conifer plantations over a five period using repeat airborne lidar datasets. They found that lidar estimated growth rates slightly underestimated the field measured growth rates. Falkowski et al. (2009) mapped forest succession using lidar metrics with an overall accuracy higher than 90%. Hudak et al. (2012) quantified AGB due to forest growth using repeat airborne lidar surveys. They developed predictive tree AGB models

using random forest algorithm and monitored biomass change using repeat discrete return airborne lidar and field surveys. They reported mean canopy height as the most significant predictor for tree biomass. Though their results suggested that biomass change and carbon dynamics in conifer forests were monitored efficiently with discrete return multi-temporal airborne lidar datasets, a few challenges concerning repeated measures using airborne lidar exist, such as differences in lidar acquisition pulse density. Yu et al. (2006) were able to measure four years of height growth of 82 Scots pines *(Pinus sylvestris)* with multi-temporal laser surveys, and they developed a tree-to-tree matching algorithm. The three change detection techniques used in their study were: (1) differencing between canopy height models; (2) comparison between canopy profile, and (3) analysis of difference between height histograms. An R-squared value of 0.68 was obtained when field measured individual tree height growth was validated against laser derived individual tree height growth. However, multi-temporal airborne laser scans poses some difficulties such as changes in flight conditions and flight path. Though very limited research has been done on AGB change estimation using lidar, several authors have discussed the potential of this technology to study forest growth (Yu *et al*., 2006; Næsset *et al*., 2013). Situations where airborne laser data cannot be used for change detection studies are described by the previously mentioned authors, and they suggest the use of TLS for future growth analysis.

The use of TLS for spatially explicit assessment of plot level forest canopy structure was examined by Henning and Radtke (2006) in leaf-off and leaf-on conditions. The authors quantified differences in characterizations obtained under the

two conditions. The comparison results of leaf-on and leaf-off provided a RMSE of 0.169 m in DBH and mean position error of 0.29 m. Their results support the applications of TLS for multi-temporal observation. However, registration of TLS data across time was not studied by the authors, but when performed could prove advantageous for multi-temporal change detection. Kaasalainen et al. (2010) and Kankare et al. (2013) analyzed the potential of TLS to measure standing tree biomass in a laboratory environment. One main drawback of local scale AGB estimates produced using field measurements or low resolution satellite imagery are the estimate uncertainties. However, TLS data allows for non-destructive and detailed modeling of individual trees. For example, Kankare et al. (2013) developed single tree based AGB models from multiple scan TLS data and reported improved accuracies for branch biomass. They input 83 TLS based variables and performed lasso regression and stepwise regression to estimate biomass. Kaasalainen et al. (2010) concluded that TLS is a promising technology for studying biomass change, and they obtained high R-squared values of 0.95 to 0.99 when TLS estimated standing tree biomass were validated with field measured biomass.

The majority of existing studies only investigate biomass estimation in static conditions, i.e., determining various forest parameters and estimating AGB at a single point in time. Thus, by utilizing multi-temporal lidar data, there is potential in increasing the scope of lidar remote sensing for carbon modeling, wildfire risk assessment, and other applications (Hudak *et al*., 2009). Biomass is dynamic and hence has to be monitored continuously to provide information on sinks and sources of carbon. It is also

essential to utilize such information to project AGB changes to inform decision making processes (Avery and Burkhart, 2002; Houghton *et al*., 2009). Until recently, measuring and monitoring forest growth were mostly done using airborne laser scanning, making change detection challenging at individual tree level. Since the potential to monitor forest growth with multi-temporal TLS datasets remains untested in current literature, this study will investigate methods to measure and monitor change in forest biomass using TLS data. We believe that the results of this study will benefit forest management and planners, and other remote sensing studies from airborne and spaceborne platforms, for map upscaling, data fusion, or calibration purposes.

Since Southern pine forests are extremely productive and bolster forest carbon sequestration capacity, regular monitoring of the forests is essential to manage the resources efficiently (Johnsen *et al*., 2001). As the non-destructive and non-contact measurements can be collected by a lidar system at multiple moments in time, the growth parameters of trees over time can be assessed (Watt and Donoghue, 2005; Dassot *et al*., 2011) with high accuracy. In addition, when extended to a larger area, the multi-temporal change study will provide us with information on tree mortality and continuous forest dynamics.

The overall goal of this research is to study tree level growth in various forest structural parameters and AGB using multi-temporal TLS datasets. Specific objectives are to (1) develop models using TLS parameters to estimate tree level AGB; and (2) investigate different conceptual approaches for estimating change in AGB.

3.2 Materials and Methods

The flowchart presented in figure 27 provides the general methodology followed to accomplish the objectives of this study.

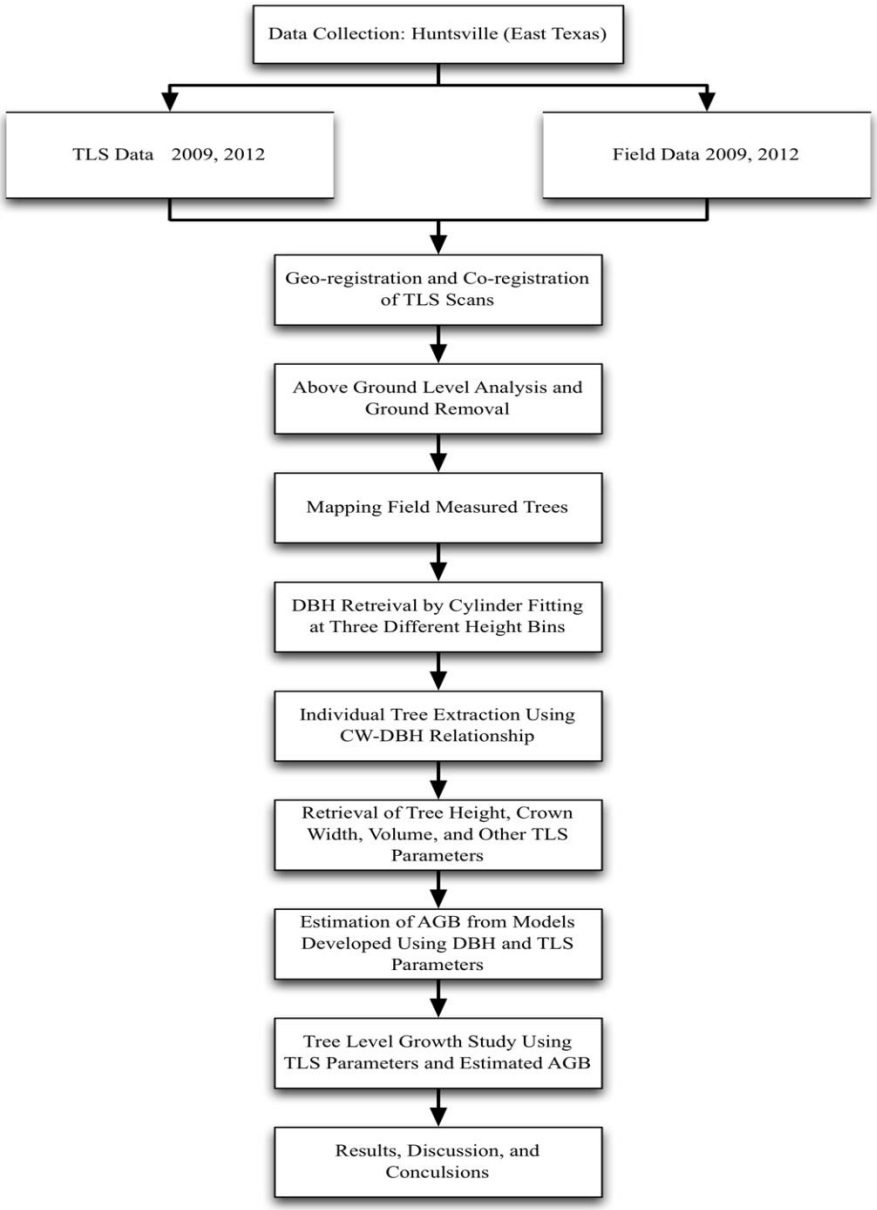

Figure 27. Methodology flowchart to study tree level growth in height, DBH, and AGB.

This section includes details of the study area, description of the data used in this study, methods used to retrieve tree level TLS parameters, estimation of tree level AGB and studying tree level growth using TLS derived forest structural parameters and estimated AGB.

3.2.1 Study Area

The study area for this research is located near Huntsville, East Texas, centered within the rectangle defined by 95°24′57″W - 30°39′36″N and 95°21′33″W - 30°44′12″N. It includes three plots; two of which cover an area of 404.600 m² (1/10th acre; r = 11.35 m) and one that covers 40.468 m² (1/100th acre; r = 3.59 m) (Figure 28). The dominant species in this site is loblolly pine (*Pinus taeda*), while other cover types in this area include upland and bottomland hardwoods, young pine plantations, and old growth pine stands. Loblolly pine is a fast growing pine extensively planted for lumber and pulpwood, being widely cultivated in the southern United States. Besides various human industrial uses for furniture, pilings, etc., it is also used as a wind break and stabilizes eroded soil. The topography of the study area is characterized by gentle slopes with elevation ranging from 62 to 105 m.

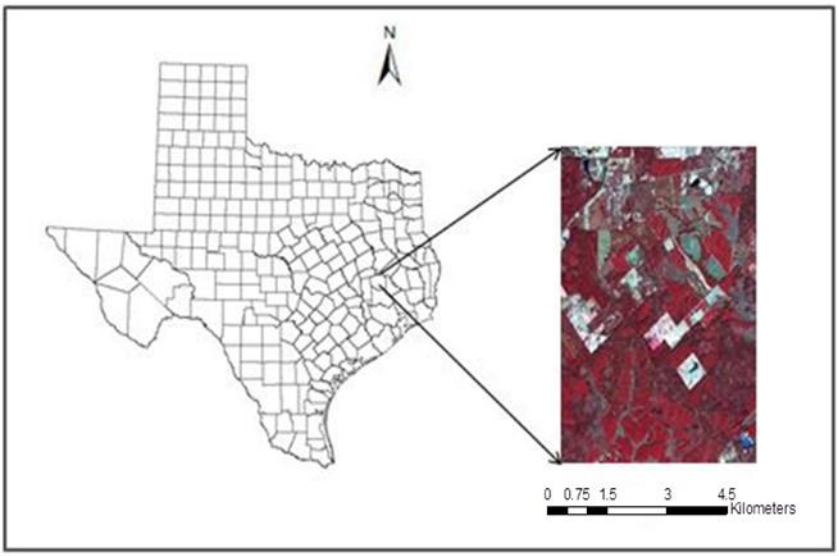

Figure 28. Study area located in Huntsville, TX shown as a false color composite of national agricultural imagery program (NAIP) image.

3.2.2 Terrestrial Laser Scanning (TLS) Data

The scans were conducted using Leica ScanStation2, a high point density 3D laser scanner, which emits visible green light pulses (532 nm) with a scan rate of 50,000 pulses per second. Single point accuracies of 4 mm for distance measurement and 6 mm for positional measurement from 1 to 50 m can be achieved with this scanner. The maximum field-of-view is 360º horizontal and 270º vertical. As commonly noted in literature, the collection of multiple scans were time consuming compared to single scan (Aschoff and Spiecker, 2004; Bienert *et al*., 2006). Hence, only single scans (360° center scans) were conducted for the three plots in November 2009 and November 2012. Two stationary reference targets were used while scanning the plots, which further allowed us to geo-register the scans. The position of the scanner was recorded using a differential global positioning system (GPS), and the azimuth to targets was measured using a

compass. Scans for the study sites were conducted with a point density of one laser pulse within 10 cm x 10 cm at a distance of 50 m. Single scan time for each plot in the study area was approximately 40 min.

3.2.3 Ground Inventory Data

Field measurements for this study included: tree species, height, DBH, crown width, and distance and azimuth from plot center. A laser technology Inc (LTI) TruPulse 360 laser range finder was used to find the distance and azimuth to each tree, and measure the tree height and crown width. A diameter tape was used to measure DBH to the nearest tenth of an inch. The coordinates of each plot center and positions of reference targets were recorded by point averaging using a wide area augmentation system (WAAS) enabled Trimble global positioning system (GPS). Post-processing of GPS data included differential correction using Trimble's Pathfinder software. Ground heights derived from a digital elevation model (DEM) were assigned to the differentially corrected points.

3.2.4 Retrieval of Tree Level TLS Parameters

The processing of TLS data is elaborated in section 2.2.4. The multi-temporal data were geo-registered and then co-registered. Above ground level (AGL) heights were computed and ground returns were filtered. Field measured trees were mapped using "Map Trees" tool (also described in section 2.2.4). The point clouds were extracted for individual trees by isolating points using a cylinder with diameter equal to an expected crown width for each tree. In this study, a relationship between field measured crown widths and DBH was established from field surveys conducted in

2004.The detailed procedure for extracting individual trees from TLS point cloud is explained in section 2.2.6. All extracted trees in the three plots were grouped into loblolly pines and hardwoods. Once the trees were extracted, the point cloud was converted into LASer file format (LAS). LAS is a public binary file format, which can manage and standardize massive size of lidar data. Tree level DBH and crown widths were derived using methods discussed in sections 2.2.5 and 2.2.7 for study site 2. Since only single scans were conducted at site 2; increased size height bins of 20 cm, 40 cm, and 60 cm were required to retrieve DBH. Zolkos et al. (2013) discussed about edge effect, where DBH extraction from remote sensing would be sensitive to any stems inside the plot boundary that have crowns extending beyond the boundary, but field measurements would not. In this study, plot level edge effects have been accounted for, because only trees in the point cloud that corresponded to the field mapped trees have been considered for DBH retrieval using cylinder fitting. Crown widths were obtained using FUSION and LDV. Measurement cylinders were set over each tree, and the diameter was adjusted to compute the crown width.

TLS parameters were derived using the command line programs of FUSION/LDV (McGaughey, 2007). A total of 22 geometric and statistical parameters were calculated from the TLS data for individual trees. TLS statistical parameters were computed using the CloudMetrics program. The output of CloudMetrics program was provided in a comma separated value (CSV) file, with one record of data for each tree LAS file processed. Total return count, maximum height, mean height, standard deviation, and variance were computed. In addition, 25^{th}, 50^{th}, 75^{th}, and 90^{th} percentiles

were computed. A robust estimator of the variability within a data sample is median absolute deviation from the median (MAD Median), which was also used an independent variable to estimate biomass.

Two other variables were computed from the crown base height (CBH): All returns above average CBH and percentage (%) of all returns above average CBH. The average CBH values were used as height breaks instead of the individual tree CBH to compute the cover estimates, in order to capture the variation in crown cover between the trees. Since field measurements for CBH were not recorded in 2009 and 2012, the average CBH was calculated from 2004 field measurements for 100 loblolly pines and 100 hardwoods as 9.91 m and 6.51 m respectively. Output values for the cover estimates ranged from 0.0 to 100.0 percent. Crown cover is an important attribute, which is used to measure tree health, and it is an approximate indicator of stand density. It provides information on the amount of plant material, such as leaves and branches that obstructs skylight from penetrating through the tree crown (Avery and Burkhart, 2002).

Upper surface area and total volume under upper surface (or between the ground and surface) were calculated using SurfaceStats program, a command line program of FUSION/LDV. Height models were created for each tree, which were given as input to this program. SurfaceStats is essential to compute the measures of canopy surface roughness and volume for small areas. Volume and surface area were calculated by separating every grid cell in the surface into two triangles, starting from the lower left to the upper right corner of the surface. The 3D coordinates of the vertices of the triangle were used to calculate the area of every triangle. The area was computed from the

magnitude of the cross product of three vertices of the triangle. Then, half of the grid cell area was multiplied by the average height of the three vertices to obtain volume under the surface for each triangle. Sum of the values for each triangle provided the totals for the entire surface.

3.2.5 AGB Estimation from Models Developed Using DBH and TLS Parameters

AGB was estimated using national (Jenkins *et al*., 2003) and species specific regional equations (Lenhart *et al*., 1987) for loblolly pines. Due to different hardwood species in the study area and lack of regional equations for each, AGB of hardwoods was estimated only using national equations. The response variable was field measured AGB, which was first calculated for loblolly pines and hardwoods using the following Jenkins's national DBH based allometric equation:

$b_m = Exp(\beta_0 + \beta_1 lnDBH)$, where

bm = total aboveground biomass (kg dry weight)

DBH = dbh for trees 2.5 cm and larger diameter at breast height (cm)

Exp = exponential function

ln = log base e (2.718282)

Jenkins et al. (2003) clearly mentioned that the published equations may be applied for large-scale estimation of AGB, but should be used carefully at very small scales. Hence, AGB was also estimated using regional equations. Lenhart et al. (1987) developed AGB equations from 65 loblolly pines in East Texas. The following regional equation was used to estimate AGB for loblolly pines:

$CTDWW = 0.060286D^{2.12686}H^{0.970500}$, where

CTDWW = complete tree dry weight in pounds of wood

D = dbh for trees 4.5 ft above ground (inches)

H = total tree height above ground (feet)

For AGB estimation using national and regional equations, the following initial set of TLS derived explanatory variables were used (Table 5):

Table 5. List of TLS parameters to estimate AGB.

TLS parameter	Description
DBH	TLS derived DBH by cylinder fitting (1.0-1.6 m height bin)
Vol	Volume under upper surface area
Area	Upper surface area
Crown width	Crown width
Total count	Total return count
Ht max	Maximum height
Ht mean	Mean height
Ht stddev	Standard deviation
Ht var	Variance
Ht CV	Coefficient of variation
Ht IQ	Interquartile distance
AAD	Average Absolute Deviation
MAD median	Median of the absolute deviations from the overall median
P25	25^{th} percentile height
P50	50^{th} percentile height
P75	75^{th} percentile height
P90	90^{th} percentile height
Canopy relief ratio	Canopy relief ratio
% returns above mean	% returns above mean
All returns above mean	All returns above mean
% returns above avg CBH	% returns above average crown base height
All returns above avg CBH	All returns above average crown base height

Four different models were developed to estimate AGB, with reference values computed separately using national and regional equations. The first model was developed by selecting variables using an initial mixed stepwise regression, in which inclusion and removal of variables were based on a significance level of 0.05. It was followed by examining the multicollinearity problem through variance inflation factor (VIF) analysis and all variables with a VIF >10 were removed from the model. The second model to estimate AGB was developed using TLS derived DBH. From section 2.3.1, since higher R-squared value, low RMSE and higher number of trees were obtained for DBH derived by cylinder fitting on 1.0-1.6 m height bin, the same was used as an explanatory variable to estimate AGB. The third model was developed only with TLS derived geometric and statistical parameters, excluding DBH. The selection of TLS parameters to estimate AGB was done based on the correlations with field measured AGB, obtained from multivariate analysis. The significant parameters with higher correlations to field measured AGB and VIF less than 10 were included in the model. The fourth model to estimate AGB was built using TLS parameters and DBH.

3.2.6 Estimation of Change in Tree Level Forest Structural Parameters and AGB for Loblolly Pines

Growth and yield modeling should be restricted to shorter time periods not exceeding 5 to 10 years, because the rate of tree growth in volume, DBH, or height is heavily influenced by tree age (Avery and Burkhart, 2002). To study forest biomass change, at least two observations over a 5 year period are required (Houghton *et al*., 2009). Biomass change over a period of 11 years was estimated by Næsset et al. (2013)

using a direct estimation approach based on field measurements and model assisted approach based on airborne lidar data as additional information. The authors related the change in biomass estimated using airborne lidar derived explanatory variables to various management activities.

The second objective of this research was to study forest growth over a period of 3 years using multi-temporal TLS data collected in 2009 and 2012. Growth in tree height was calculated as the difference between the TLS derived heights for 2009 and 2012. Scatterplots for DBH and height with height growth were developed to study the trend in height growth with increasing height and DBH. Field measured AGB growth was also studied as a function of tree height. To estimate the change in AGB, three different approaches were followed. The first approach was to estimate AGB change by modeling AGB for 2009 and 2012 simultaneously, with field and TLS data available for both years. Models for AGB were fitted separately. Change in AGB was calculated as the difference between the estimated AGB for 2009 and 2012. The second approach was separate modeling of AGB for 2009 and 2012, but in this case, field and TLS data were available for 2009; only TLS data was considered available for 2012. AGB estimation models were built using the data from 2009. AGB for 2012 was estimated using the model developed from 2009 field and 2012 TLS data. Then, AGB change was the difference between the estimated AGB for 2009 and 2012. The rationale for this second approach was based on remote sensing paradigm of reducing but not eliminating field work, by using previously developed models to update remote sensing estimates of biophysical parameters, in this case biomass. The third approach was the direct modeling

of AGB change, in which the changes in TLS parameters were used as independent variables. Unlike the first two approaches, the results from direct modeling approach are affected by only one model error (Bollandsås *et al.*, 2012). The purpose of estimating AGB change using the third approach was to investigate whether forest growth can be studied independent of field data, thereby minimizing manual labor and time. The three approaches used to model AGB change are shown in figure 29.

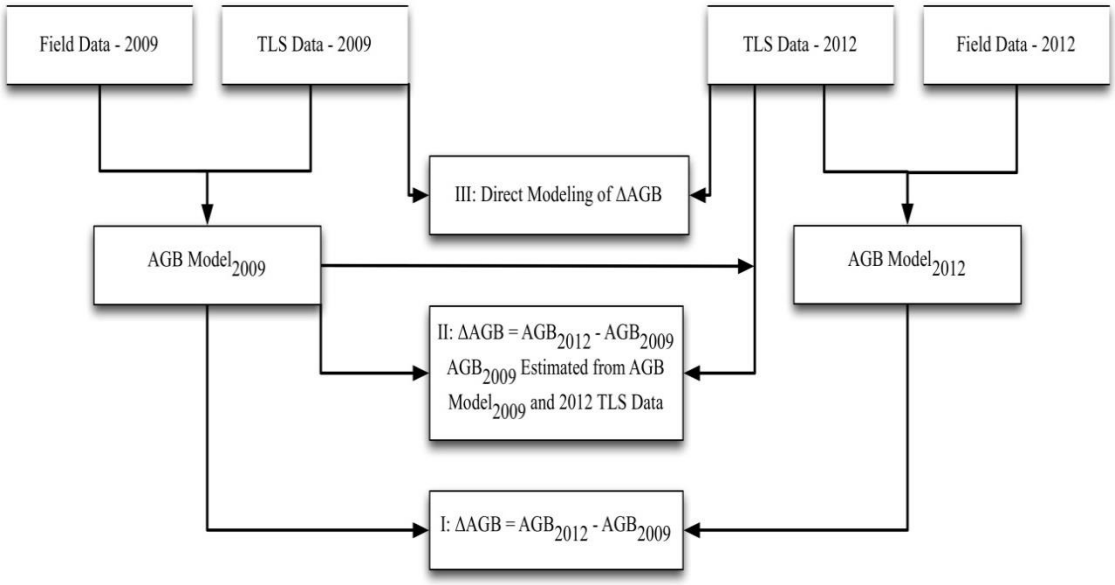

Figure 29. Three approaches used to estimate AGB change.

Dubayah et al. (2010) identified carbon sources and sinks by observing changes in the various height metrics and biomass derived from multi-temporal medium altitude waveform lidar data. The authors discussed the need for better allometric equations to estimate biomass, since DBH based allometric equations may contain errors as they are

developed from limited number of trees, thus failing to provide accurate biomass estimates. Thus, for each approach, different models were developed using TLS derived DBH, geometric and statistical parameters.

3.3 Results and Discussion

3.3.1 Tree Level AGB Estimation for Loblolly Pines and Hardwoods

The distribution of 58 loblolly pine trees by DBH and height classes is shown in figure 30. It can be seen that the DBH for most of the trees ranged from 12 to 27 cm, with only two larger trees whose DBH were greater than 30 cm.

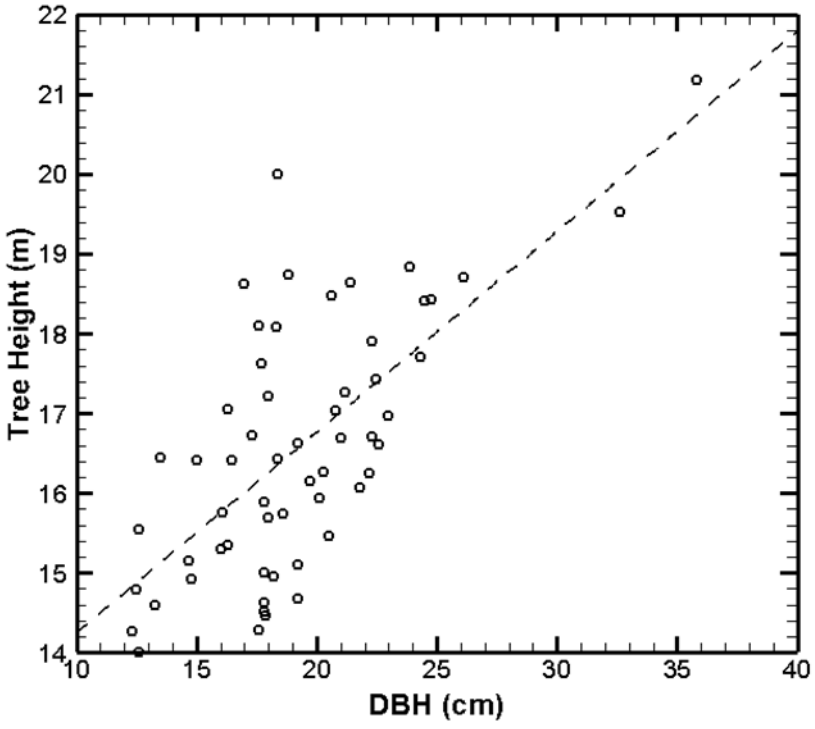

Figure 30. Distribution of height and DBH for 58 loblolly pines.

Tables 6 and 7 show the correlations of various TLS geometric and statistical parameters with field measured AGB calculated using national and regional equations respectively. It can be seen from tables 6 and 7 that TLS derived geometric parameters such as DBH, volume, area, and crown width were better correlated with field measured biomass compared to TLS derived statistical parameters. Our results agree with the findings of Kankare et al. (2013), who reported that the best correlations between TLS based features and biomass components were achieved with the measured geometric features that are less dependent on scanning parameters such as lidar point densities compared to statistical parameters. Parameters such as percent returns above mean, total count, and percent returns above average CBH were poorly correlated with field measured AGB. Presence of heavy understory in 2012 plots, which obstructs the penetration of TLS pulses completely to reach the trees could be one of the reasons for the weak relationship between few statistical parameters and field measured AGB.

Table 6. Correlations of TLS parameters with field measured AGB for loblolly pines and hardwoods calculated using national equations.

Loblolly Pines		Hardwoods	
Parameter	Correlation	Parameter	Correlation
DBH	0.9648	Vol	0.9910
Crown width	0.8552	Area	0.9608
Vol	0.7712	DBH	0.9389
Ht max	0.6561	Ht var	0.9194
Area	0.6382	Crown width	0.8853
Returns above avg CBH	0.4101	P90	0.8613
Returns above mean	0.4003	P25	0.8571
Total count	0.3826	Ht mean	0.8469

Table 6. Continued

Loblolly Pines		Hardwoods	
Parameter	Correlation	Parameter	Correlation
Ht var	0.3316	P50	0.8434
P90	0.3306	P75	0.8430
Ht stddev	0.3271	Ht max	0.8400
AAD	0.2458	Ht stddev	0.8293
Ht mean	0.1493	AAD	0.7636
% returns above avg CBH	0.1427	Returns above avg CBH	0.6601
P25	0.1419	MAD median	0.6132
Ht CV	0.1403	Ht IQ	0.6004
P50	0.1315	Returns above mean	0.4836
P75	0.0972	% returns above avg CBH	0.4451
% returns above mean	-0.0094	Total count	0.4445
Ht IQ	-0.0442	Ht CV	0.3141
Canopy relief ratio	-0.1014	% returns above mean	0.2404
MAD median	-0.1411	Canopy relief ratio	-0.1494

Table 7. Correlations of TLS parameters with field measured AGB calculated for loblolly pines using regional equations.

Parameter	Correlation
DBH	0.9570
Crown width	0.8398
Vol	0.7673
Ht max	0.7205
Area	0.6440
Returns above avg CBH	0.4390
Returns above mean	0.4289
Total count	0.4113
Ht var	0.3807
Ht stddev	0.3695
P90	0.3505
AAD	0.2855
Ht CV	0.1704
Ht mean	0.1507
% returns above avg CBH	0.1389

Table 7. Continued

Parameter	Correlation
P50	0.1338
P25	0.1260
P75	0.1110
Ht IQ	-0.0114
% returns above mean	-0.0188
Canopy relief ratio	-0.1235
MAD median	-0.1313

The four different AGB estimation models for loblolly pines based on national and regional equations are given in tables 8 and 9 respectively. The parameters and coefficients for each model are also included in the tables. Both national and regional level AGB estimation models based on the results from stepwise regression had TLS derived DBH and interquartile distance as independent variables. Variance was an additional independent variable in the national level AGB estimation model. DBH is an important forest inventory attribute because it serves as a fundamental parameter in tree allometry, providing valuable information about individual trees and the forest stand structure (Moskal and Zheng, 2012). Interquartile range and variance are measures of statistical dispersion, which relates to the structure of a tree by providing information on the stretch of a distribution.

Based on the results of the third model developed from TLS parameters, both national and regional level AGB estimation models had the same independent variables in the models: crown width, maximum height, and 50^{th} percentile. Crown width (CW) is an important variable, which can be used to estimate biomass, tree volume, and leaf area

(Evans *et al*., 2006). Extensive literature studies revealed that crown width had so far not been estimated from TLS data and a limited number of studies had derived crown width from airborne lidar data (Popescu *et al*., 2003; Evans *et al*., 2006; Van Leeuwen and Nieuwenhuis, 2010). Thus, to our knowledge, the results from this study will be the first to develop AGB estimation model using TLS derived crown width as an independent variable. The second variable in the model, tree height is also a vital parameter, which provides qualitative information about the plot or stand and quantitative information about the tree. DBH and tree heights are positively correlated with biomass, since stem diameter increases as trees grow taller, thus increasing the amount of foliage supported by the trees (Dubayah and Drake, 2000). The third variable in the model is the 50^{th} percentile height or median, which is the height of median energy (HOME), an important variable used to derive forest structural parameters and estimate AGB from waveform lidar data (Drake *et al*., 2002; Zhao *et al*., 2013).

For the final model developed using TLS parameters and DBH, interquartile distance and maximum height were independent variables for the national and regional level AGB estimation models respectively in addition to TLS derived DBH. Though it can be seen from table 6 that interquartile distance was not highly correlated to field measured AGB, it was the only significant parameter along with DBH with a VIF less than 10. On the other hand, maximum height had a higher correlation of 0.7205 with field measured AGB calculated from regional equation (Table 7).

Table 8. Model parameters and coefficients for the estimation of AGB for loblolly pines based on national equation.

Model	Parameters and coefficients
Stepwise regression	15.03(DBH)+2.48(Ht var)-9.17(Ht IQ)-161.23
DBH	16.56(DBH)-197.69
TLS parameters	82.50(Crown width)+10.24(Ht max)-5.85(P50)-284.84
TLS parameters+DBH	16.63(DBH)-2.52(Ht IQ)-186.31

Table 9. Model parameters and coefficients for the estimation of AGB for loblolly pines based on regional equation.

Model	Parameters and coefficients
Stepwise regression	15.61(DBH)-1.51(Ht IQ)-181.21
DBH	15.57(DBH)-188.03
TLS parameters	70.03(Crown width)+14.53(Ht max)-4.83(P50)-331.02
TLS parameters+DBH	14.16(DBH)+5.60(Ht max)-188.03

The results obtained for AGB estimation for 58 loblolly pines using models developed based on national and regional equations were compared (Table 10) to see if national or regional based models provided accurate estimations of AGB. Though the adjusted R-squared values and RMSE for four different models based on national and regional equations were not considerably different, results showed that national level AGB models performed better than regional level AGB models except for the model developed using TLS parameters alone. Thus, in AGB change estimation for loblolly pines, field measured AGB estimated using the national equation was to develop the models (section 3.3.2).

Table 10. Comparison of AGB estimation models based on national and regional equations for loblolly pines.

Model	National level AGB models		Regional level AGB models	
	Adjusted R^2	RMSE (kg)	Adjusted R^2	RMSE (kg)
Stepwise regression	0.95	15.99	0.92	20.52
DBH	0.93	19.85	0.91	20.74
TLS parameters	0.82	31.33	0.83	28.81
TLS parameters+DBH	0.94	18.81	0.92	19.82

Figure 31 shows the distribution of field measured AGB calculated using national equation for loblolly pines and distributions of estimated AGB from four different models as explained above. Though the mean estimated AGB from the four models were the same as the mean field measured AGB, results from table 10 and figure 31 showed that the best AGB estimation model was the one developed using the variables selected from stepwise regression, with the highest adjusted R-squared value and lowest RMSE.

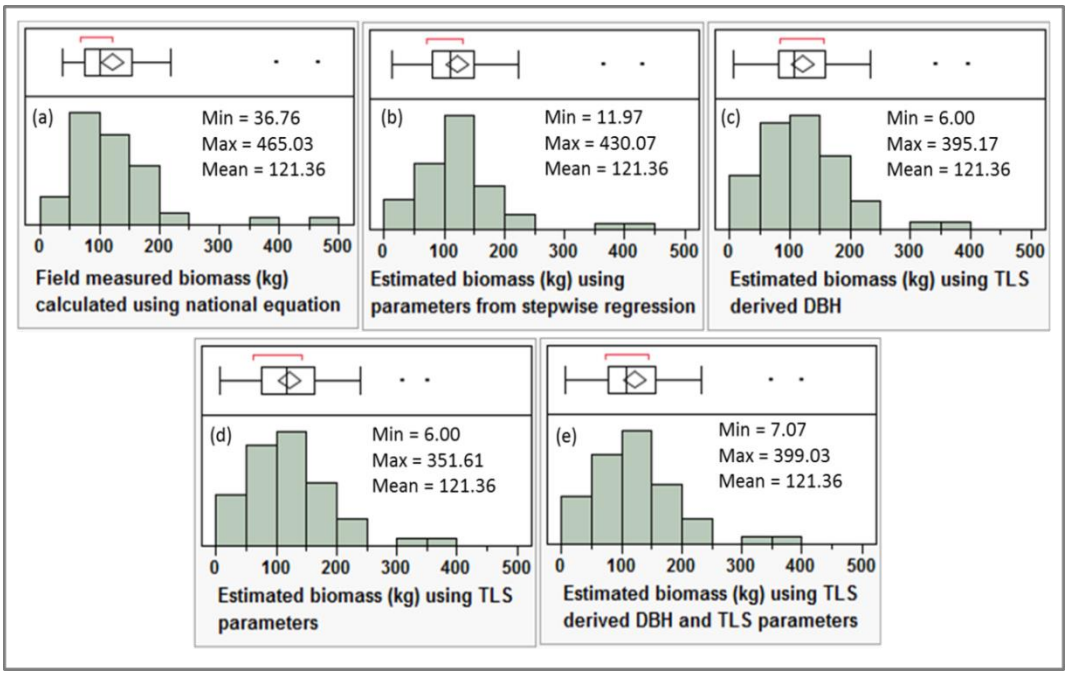

Figure 31. Frequency distributions of field measured AGB for loblolly pines based on national equations and estimated AGB using four different models.

For hardwoods, only models based on national equation were developed. Table 11 provides the various models with the respective parameters and coefficients. The third model built using TLS parameters had a significantly high R-squared value of 0.99 and low RMSE value of 32.33. Volume and crown width were the independent variables, which had high correlation values of 0.9910 and 0.8853 with field measured AGB (Table 6).

Table 11. Model parameters and coefficients for the estimation of AGB for hardwoods based on the national equation.

Model	Parameters and coefficients
Stepwise regression	21.54(DBH)+37.94(Crown width)+2.78(Ht mean)+ 6.59(% returns above mean)-708.70
DBH	30.88(DBH)-294.79
TLS parameters	1.30(Vol)-35.60(Crown width)+69.45
TLS parameters+DBH	38.71(DBH)-108.99(MAD median)-224.77

Figure 32 shows the distribution of field measured AGB calculated using the national equation for hardwoods and distributions of estimated AGB from four different models. The results were in agreement with those from table 12 that the model developed using TLS parameters performed the best compared to other three models.

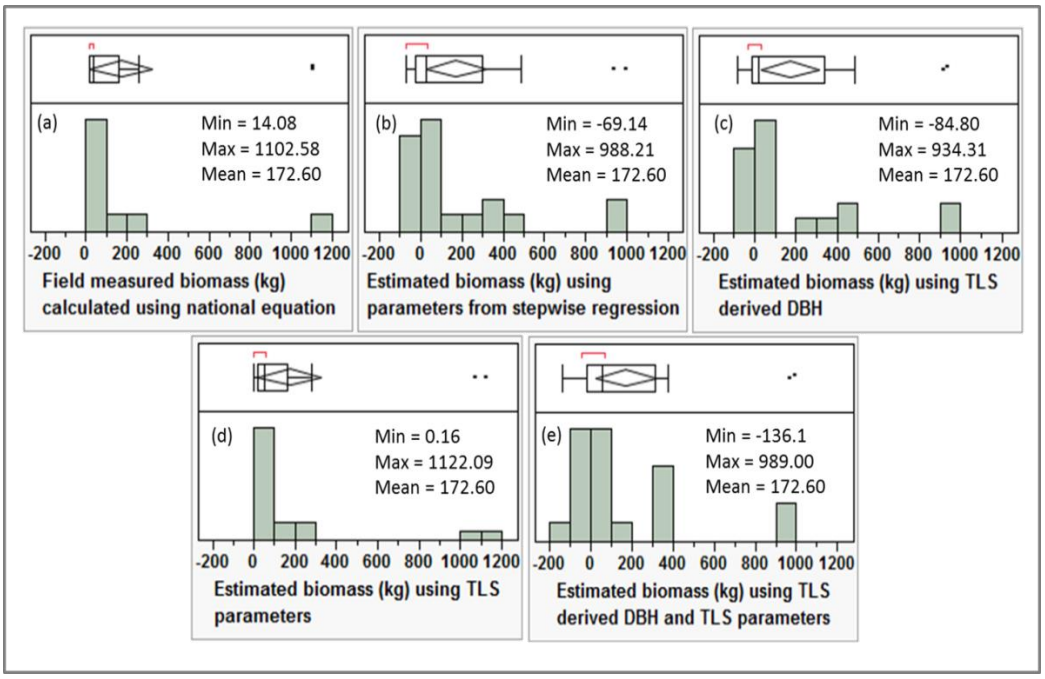

Figure 32. Frequency distributions of field measured AGB for hardwoods based on national equation and estimated AGB using four different models.

Table 12. Salient model results for the estimation of AGB for hardwoods based on national equations

Model	Number of trees	Adjusted R^2	RMSE (kg)
Stepwise regression	20	0.88	111.70
DBH	20	0.87	115.62
TLS parameters	20	0.99	32.23
TLS parameters+DBH	20	0.91	99.01

Though the maximum estimated AGB was close to the field measured AGB, a negative minimum estimated AGB was obtained from the three models excluding the one built using TLS parameters only. This means that the AGB decreased from 2009 to 2012, which was not true as observed from field measured AGB results. The reason for the underestimation of AGB in 2012 for a few trees might be due to canopy shadowing, in which case TLS pulses would not have penetrated completely to certain parts of the individual trees due to heavy understory. Canopy architecture is a significant parameter which largely influences the penetration of laser pulses. AGB was overestimated for a few trees in 2009 and the reason could be due to the inability to separate tree crowns completely for plots with heavy overstory.

3.3.2 Tree Level Growth for Loblolly Pines

Stukey (2013) established a relationship between age and lidar estimated tree height through site index. The individual tree age for loblolly pines in Huntsville was estimated using 2004 airborne lidar data. An R-squared value of 0.99 was obtained when the average field age in 2004 were regressed against average age predicted using lidar estimated heights for ten plots. Loblolly pines identified using TreeVaW (Tree Variable Window) software were provided by Stukey. Each tree had various attributes including

the estimated age from lidar derived heights and site index. For our study, the trees in three plots used to estimate tree level change were extracted from the entire study area. When the field measured trees were mapped on the TreeVaW identified trees, it was observed that only 70 percent of the total field measured trees were identified by TreeVaW. The estimated age for trees used to study tree level change ranged from 15 to 21 years of age in 2009 and 18 to 24 years of age in 2012. Overestimation or underestimation of age could be due to errors site index.

When height growth from 2009 to 2012 for 29 loblolly pines was plotted against field measured tree heights and DBH separately (figure 6 and 7), a meaningful relationship in height growth was not observed with increasing heights and DBH. Since most of the sample trees had DBH ranging from 14.8 to 26.1 cm, and only two trees with DBH 32.6 and 35.8 cm, a better relationship could be obtained if more trees covering a wide range of tree heights were sampled. Further, a rapid growth in height was not noticed because growth in tree height proceeds slowly in the beginning years after the establishment of the seed, which is then followed by very quick growth during the next 20 to 30 years. In addition, age is not the only variable that influences the rate of diameter and height growth. When the trees are closely spaced, root-growing space decreases resulting in smaller crowns with a decreased diameter and height growth (Avery and Burkhart, 2002). The other reason for observing a slow height and diameter growth in loblolly pines could be attributed to the presence of hardwoods in a few of our study plots. Hardwoods compete with loblolly pines for soil moisture, nutrients and other factors (Clason, 1978; Miller *et al*., 1991).

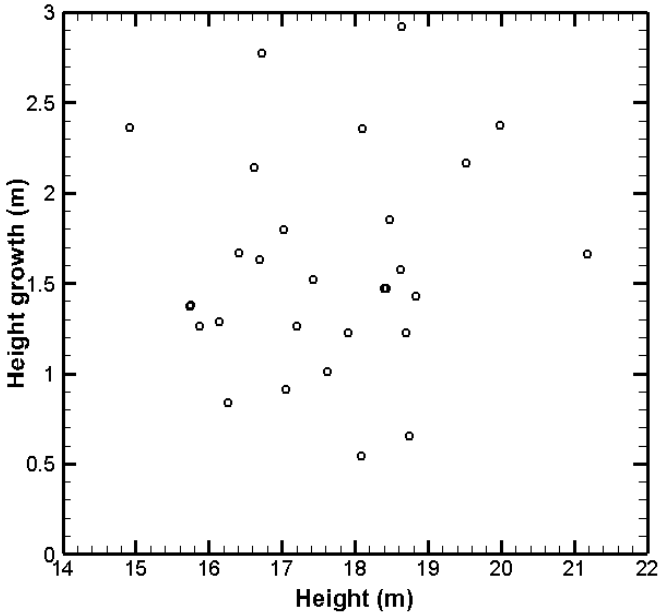

Figure 33. Scatterplot of height growth and height.

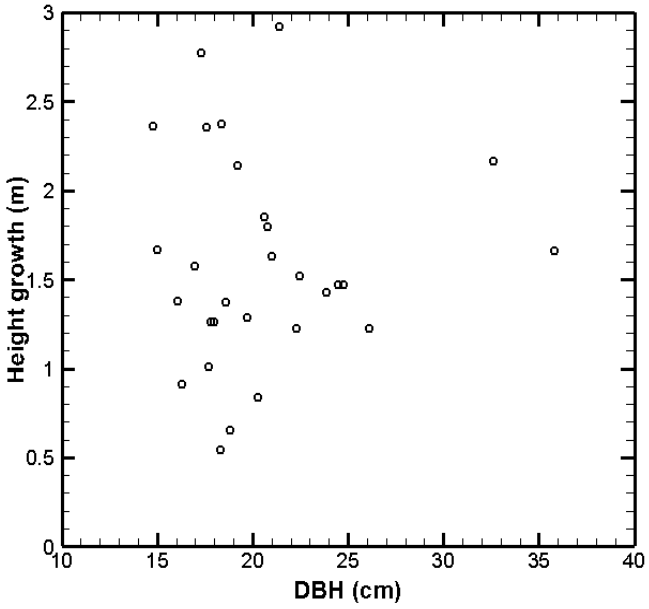

Figure 34. Scatterplot of height growth and DBH.

When change in AGB between 2009 and 2012 was plotted against tree height (Figure 35), it was seen that taller trees had an increased growth in AGB because the age of the trees used to study AGB change ranged from 15 to 24. Since canopy properties and growth are significantly related to each other, developing models to estimate change in forest structural parameters and AGB on a larger scale will be important for stand management (Dean and Baldwin, 1996).

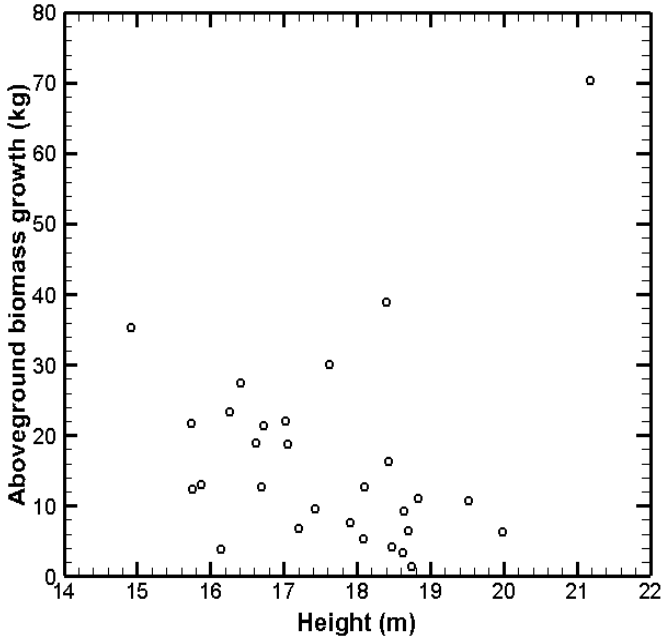

Figure 35. Scatterplot of AGB growth and height

Figure 36 shows the AGB change estimation results from approach I. Mean AGB change estimated using three different models in approach I were the same as the field measured AGB change. Minimum field measured AGB change was 1.29, but a negative

minimum AGB change was observed in the three models. The negative value for AGB change might not have necessarily been due to the decrease in AGB. The reasons might be due to the underestimation of AGB in 2012 because of canopy shadowing or overestimation of AGB in 2009 due to the inability to separate the crowns of adjacent trees completely. It is challenging to isolate individual tree crowns accurately in closed canopies due to overlapping branches of adjacent trees (Hudak *et al*., 2009). Amongst the three models, AGB change estimated using the models developed from TLS derived DBH was closest to field measured AGB change.

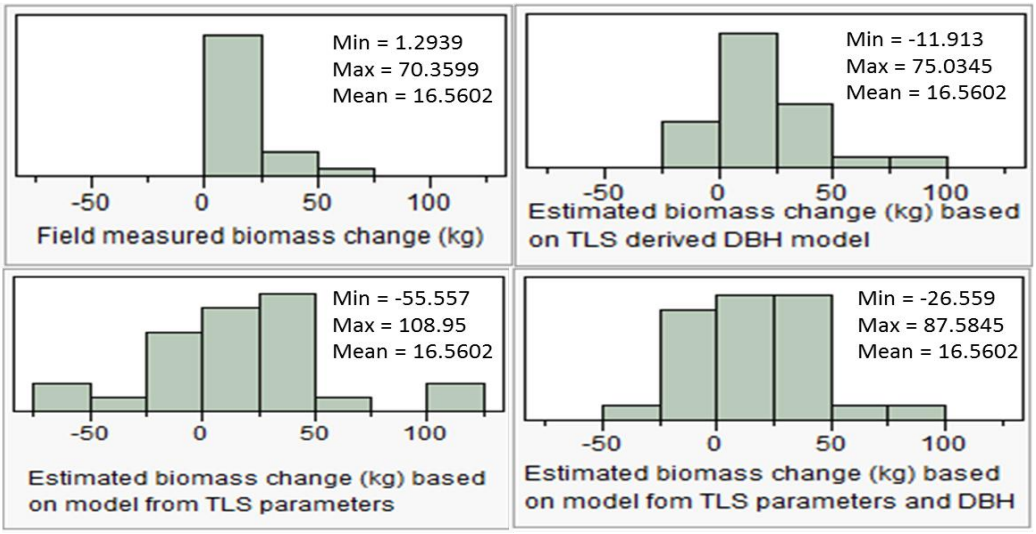

Figure 36. Distributions of AGB change using approach I.

The best models used to estimate AGB in 2009 and 2012 are given below:

$$AGB_{2009} = 15.69(DBH) - 179.21$$

$$AGB_{2012} = 17.48(DBH) - 467.65$$

AGB change was obtained by subtracting the estimated AGB in 2009 and 2012. The relationship between field measured AGB change and predicted AGB change using approach I is shown in figure 37.

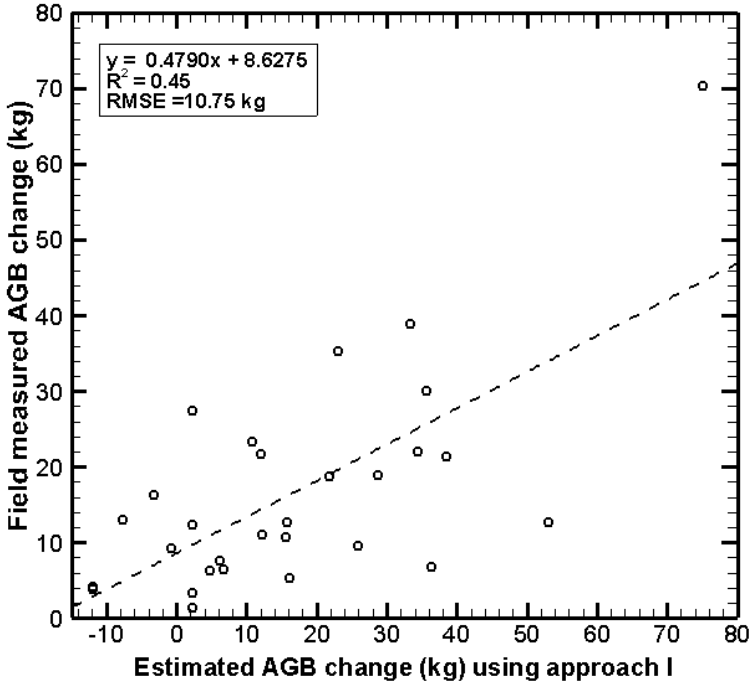

Figure 37. Regression of field measured AGB change and estimated AGB change using approach I.

AGB change estimation results from approach II are presented in figure 38. Minimum estimated AGB changes for the three models were better than the results from approach I, since a large negative AGB change was not observed. However, mean estimated AGB change for the three models were different from the field measured mean AGB change, the maximum difference being 39.44 kg and minimum difference being

3.57 kg. In this approach, the model developed using TLS derived DBH performed better compared to the other two models.

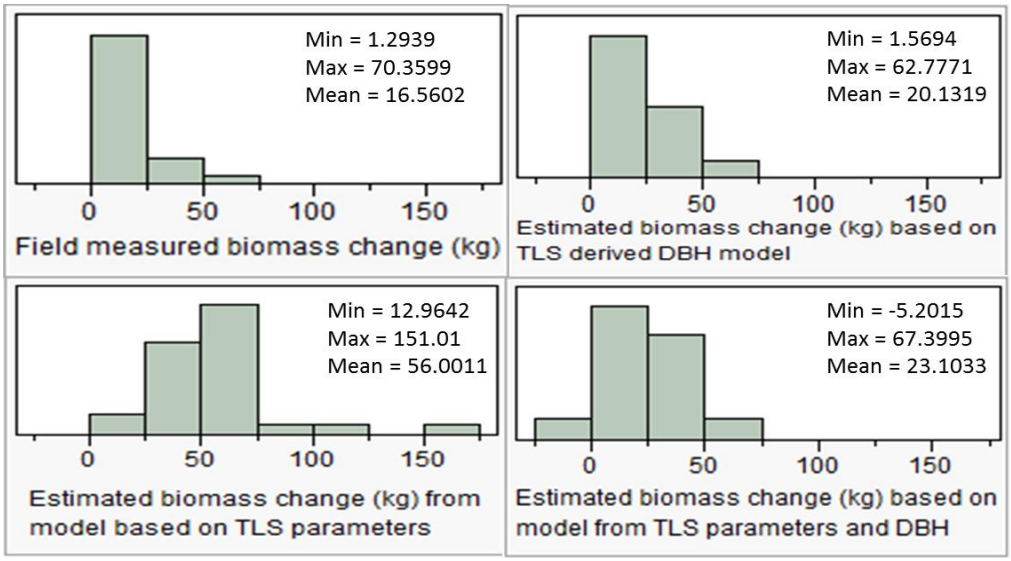

Figure 38. Distributions of AGB change using approach II.

The best model used to estimate AGB in 2009 is given below:

$$AGB_{2009} = 15.69(DBH) - 179.21$$

AGB in 2012 was obtained using the AGB model developed in 2009 and TLS data in 2012. The relationship between field measured AGB change and predicted AGB change using approach II is shown in figure 39.

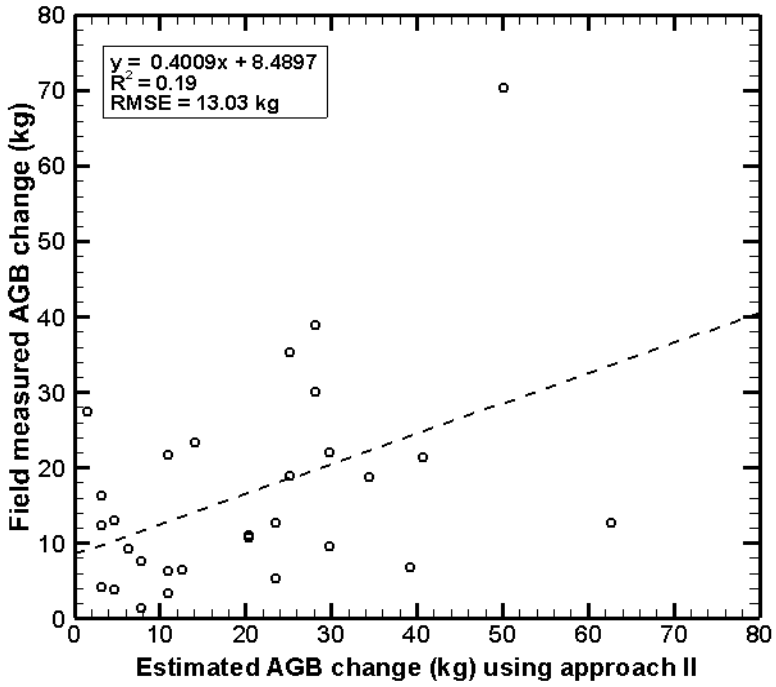

Figure 39. Regression of field measured AGB change and estimated AGB change using approach II.

Table 13 shows the correlations of change in TLS parameters with the change in field measured AGB. The change in each parameter is denoted as d(parameter), which is the difference between TLS parameters in 2009 and 2012. Change in volume and area had the highest correlations with change in field measured AGB. Though we used field measured AGB change as a dependent variable in approach III, AGB change can be estimated using these models if multi-temporal TLS datasets are alone available, thus eliminating field measurements.

Table 13. Correlations of change in TLS parameters with change in field measured AGB for loblolly pines.

Parameter	Correlation
d(Vol)	0.6122
d(Area)	0.5845
d(P25)	0.4931
d(DBH)	0.4346
d(% returns above mean)	0.3873
d(Crown width)	0.3812
d(Returns above avg CBH)	0.3767
d(Returns above mean)	0.3731
d(Total count)	0.3341
d(P50)	0.2271
d(Ht mean)	0.1884
d(% returns above avg CBH)	0.1774
d(P75)	0.1270
d(Canopy relief ratio)	0.1194
d(Ht max)	0.1074
d(Ht var)	-0.1437
d(AAD)	-0.1530
d(Ht stddev)	-0.1659
d(MAD median)	-0.1714
d(P90)	-0.1767
d(Ht IQ)	-0.2349
d(Ht CV)	-0.3005

Figure 40 shows the AGB change estimation results from approach III. The minimum estimated AGB change were better compared to the results from approach I, since a large decrease in AGB from 2009 to 2012 was not observed. Though the mean estimated AGB change from the three models was the same as the field measured AGB change, the maximum estimated AGB change was not the same. Maximum field estimated AGB change differed from the maximum AGB change estimated from the

models based on TLS derived DBH, TLS parameters, TLS parameters and DBH by 36.7039 kg, 13.7256 kg, and 23.0672 kg respectively. The best model in this approach was the one developed using TLS parameters: change in volume and change in 90^{th} percentile.

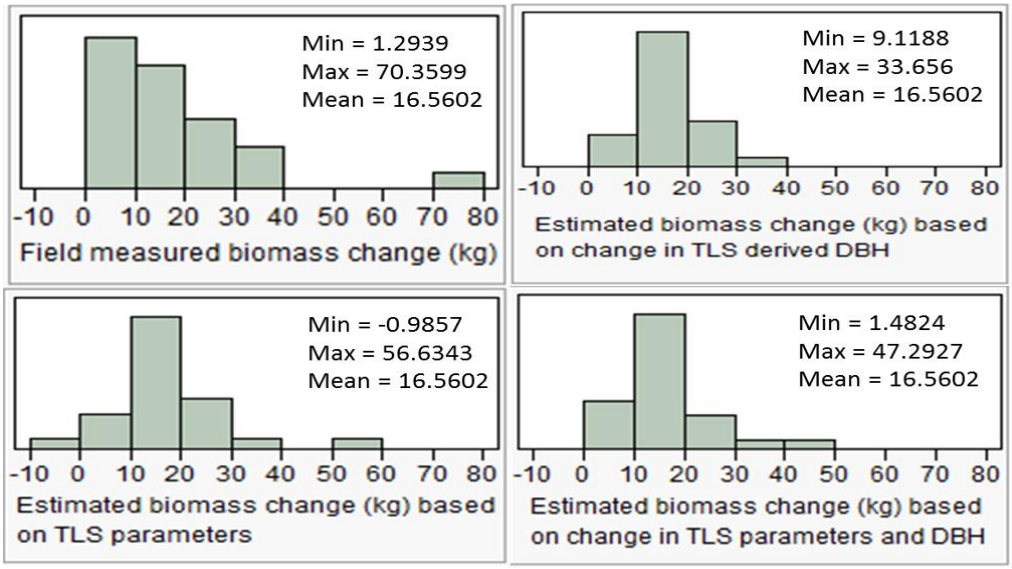

Figure 40. Distributions of AGB change using approach III.

The best model used to estimate AGB change directly using TLS datasets available in 2009 and 2012 is given below:

$$AGB\ Change = 0.15(Vol) - 1.60(P90) + 16.00$$

The relationship between field measured AGB change and predicted AGB change using approach III is shown in figure 41.

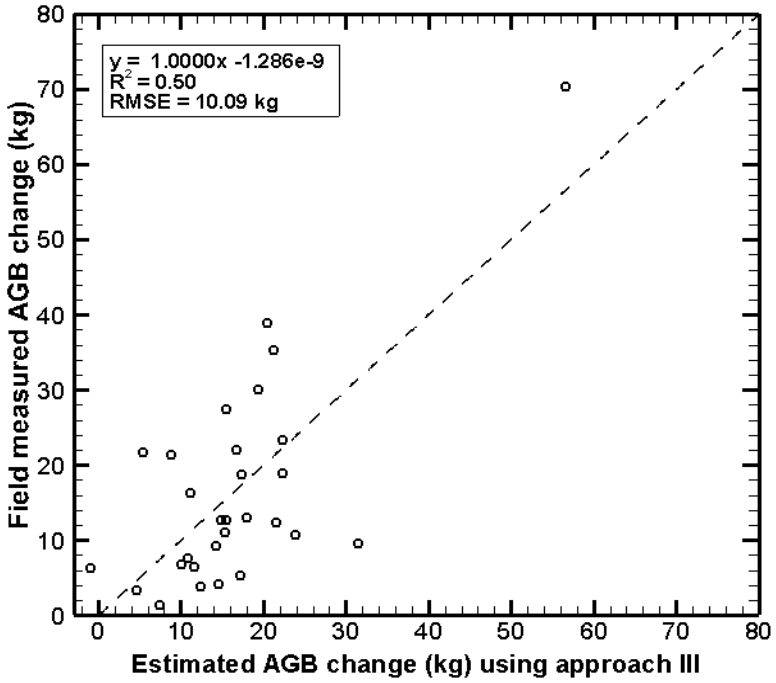

Figure 41. Regression of field measured AGB change and estimated AGB change using approach III.

Figure 42 shows the min/mean/max graph for the best AGB change estimation model using each approach compared to field measured AGB change. The model results of estimated AGB change using the three approaches are given in table 14. Though the minimum and maximum AGB changes were close to field measured AGB change, approach II had the lowest R-squared value and the highest RMSE. For most of the trees, approach II overestimated the field measured AGB change. Since AGB models developed in 2009 were used with TLS data in 2012 in approach II to estimate the AGB in 2012, errors in the estimated AGB change may be due to the following reasons: (1) differences in point densities between the 2009 and 2012 TLS scans; (2) tree shadowing due to branches of other trees or heavy understory; (3) scanner positioning errors; and

(4) errors in field measured AGB itself. The results from approach II suggests that uncertainties in AGB change estimates are possible if AGB model from one year and TLS data of the second year are used to estimate the AGB for the second year. The errors in AGB change estimates can be minimized if the scanner is placed at the same position in both years, if the same scan resolution is used, and if multiple scans are conducted to eliminate tree shadowing as much as possible.

An R-squared value of 0.45 and RMSE of 10.75 kg were obtained when field measured AGB change was regressed against estimated AGB change using approach I. However, 17 percent of the trees had a negative estimated AGB change. The underestimation of AGB change using approach I may be because of occlusion due to heavy understory in 2012, thus minimizing the complete penetration of laser pulses to reach the trees. The R-squared value and RMSE did not change significantly even when the negative estimated AGB change were changed to zero AGB change (assuming that a decrease in AGB did not occur between 2009 and 2012), and then regressed against field measured AGB change. Further, the results of estimating the AGB change by modeling AGB separately for the two years are affected by two model errors (Bollandsås *et al*., 2012).

AGB change estimations using approach III were better compared to approaches I and II. An R-squared value of 0.50 and RMSE of 10.09 kg were obtained when field measured AGB change was regressed against estimated AGB change using approach III. Large negative AGB change was not observed in approach III. Results from the direct modeling approach suggest that AGB change can be modeled independent of field

measurements, if multi-temporal TLS datasets are available. Unlike the first two approaches, the results from direct modeling approach are affected by only one model error (Bollandsås *et al*., 2012).

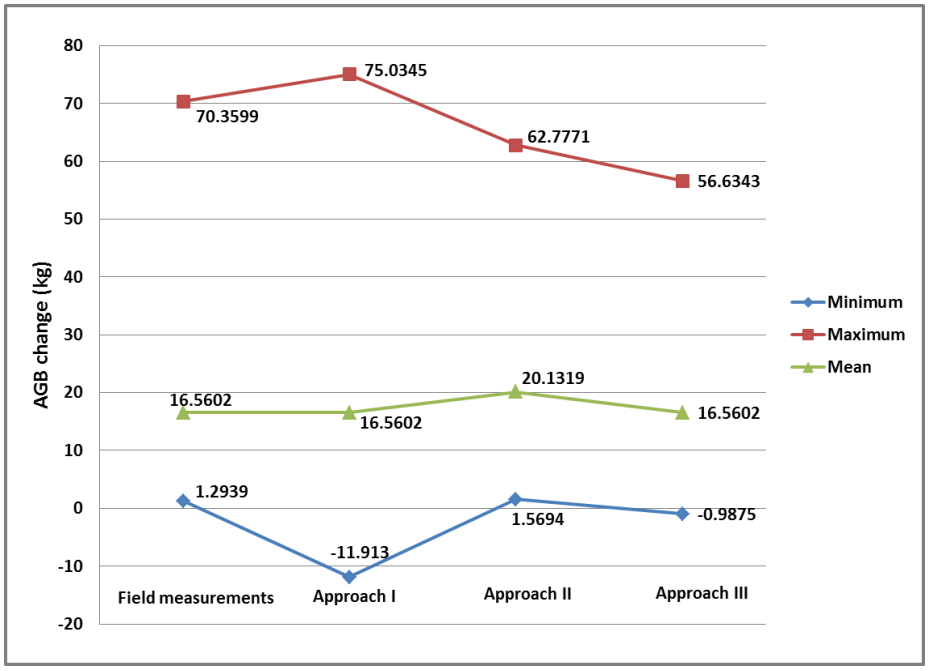

Figure 42. Min/mean/max graph for field measured AGB change and AGB change estimated using the best model of each approach.

Table 14. Model results for the estimation of AGB change for loblolly pines.

	Number of trees	R^2	RMSE (kg)
Approach I	29	0.45	10.75
Approach II	29	0.19	13.03
Approach III	29	0.50	10.09

3.4 Conclusion

TLS is a powerful technology that provides highly dense point cloud data, from which various geometric and statistical parameters can be extracted for individual trees (Kankare *et al*., 2013). Since majority of the AGB estimation models are developed only using DBH, we investigated the potential of TLS by extracting various geometric and statistical parameters for AGB estimation. This study presented different methods and statistical approaches to estimate AGB and model the change in AGB using multi-temporal TLS data. The best AGB estimation model for loblolly pines had DBH, height variance, and interquartile distance as independent variables. The best AGB estimation model for hardwoods included volume and crown width as independent variables, both being TLS geometric parameters. Since the mean estimated AGB from the models were not statistically different from the field measured AGB, these models could be used to obtain non-destructive measurements AGB for loblolly pines and hardwoods. An interesting finding was that AGB estimates for pines obtained from generalized biomass equations and regional biomass equations were not significantly different. Tree shadowing is an important factor that has to be considered and minimized in case of single scan data to prevent the underestimation or overestimation of the derived statistical parameters. For example, 50^{th} percentile or HOME, an important variable used to estimate AGB may be influenced by the laser penetration through the canopy, and the value will be higher in areas where lower portions of the canopy are shadowed due to heavy understory. Multiple scans can be conducted to avoid laser shadows as much as possible due to branches or heavy understory. Co-registered airborne lidar data can also

be integrated with terrestrial lidar data to obtain an enhanced characterization of the canopy, which may further prevent the underestimation of certain TLS derived parameters such as tree height, 75^{th} percentile, and 90^{th} percentile. Although we presented methods to estimate AGB only for loblolly pines and hardwoods, they can be applied to other tree species also.

Current and future changes in forest structural parameters and AGB are vital for prudent decision making as well as choosing appropriate growth and yield models. Natural areas can be protected by increasing the yield on fewer acres of natural stands of loblolly pines, thus minimizing the conversion of natural acres to plantations (Bruce and Bailey, 2001). We did not observe a significant relationship between growth in tree height and DBH to field measured heights. Some factors that influenced the growth of loblolly pines were competition due to hardwoods, age of the trees and spacing between the trees. Regarding AGB change, we did not model the change for hardwoods due to the lack of sufficient trees to develop the model. For AGB change of loblolly pines, approach III (Direct modeling of AGB change with TLS data available for 2009 and 2012) provided the best results. Since the mean estimated AGB changes using the direct modeling approach were not significantly different from the field measured AGB change, forest growth could be studied independent of any field measurements when biomass models are already available. However, the models could be improved by incorporating more trees with a wide range of DBH and tree heights. Negative estimated AGB change using approach I were observed for a few trees (Separate modeling of AGB to estimate AGB change) due to canopy shadowing. The results from approach II

(Models developed for 2009 from field and TLS data to estimate biomass in 2012 based on 2012 TLS data only and 2009 biomass models) overestimated the field measured AGB change for most of the trees. Such errors could be minimized by conducting multiple scans. Though a very significant relationship was not observed between the field measured AGB change and TLS estimated AGB change using the three approaches, there are no other studies we can compare results to. An extensive literature review reveals that this is the first study to model the change in AGB using different innovative and conceptual approaches with multi-temporal TLS data.

The results of our study indicate the capability of terrestrial lidar to model the change in tree level forest structural parameters and AGB, with potential for reducing the amount of field work when using multi-temporal terrestrial lidar datasets. To model change in forest structural parameters and AGB at larger scales, multi-stage sampling could be implemented based on the availability of airborne lidar data. Reliable information on tree level growth on a larger scale will also be vital to forest fire managers to make critical decisions on clearing the accumulated fuel. Monitoring various forest attributes and biomass using terrestrial and airborne lidar can further be used to validate measurements from imminent spaceborne lidar missions (Dubayah and Drake, 2000; Falkowski *et al*., 2010).

CHAPTER IV

SUMMARY AND CONCLUSIONS

The efficacy of terrestrial lidar in retrieving different forest structural parameters rapidly and accurately at an individual tree level using novel methods was clearly demonstrated in this study. Some of the new methods implemented in this study were cylinder fitting on three different height bins to retrieve DBH, tree mapping using an automatic tool developed in ArcObjects, extracting individual trees from TLS point clouds to retrieve tree height and crown width, and investigating the influence of the number of scans on DBH estimation accuracy.For site 1, due to two-direction scans and adequate laser point densities in the 1.2-1.4 m height bin, increased height bin size for cylinder fitting may not be required to retrieve DBH. For the circular plots at site 2, cylinder fitting with increased height bin size provided improved accuracies for DBH estimates from single scan TLS data. A high R-squared value of 0.97 and RMSE of 1.85 cm were obtained when DBH retrieved by cylinder fitting on 1.0-1.6 m height bin were validated against field measured DBH. For site 1, the mean height decreased from 2010 to 2012 due to leaf-on and leaf-off scans respectively, while individual tree level heights increased from 2010 to 2012. For site 2, as leaf-on scans were conducted for both the years, tree height increased from 2009 to 2012. The R-squared value was 0.84 when field measured crown widths were validated against TLS derived crown widths. Underestimation of field measured crown widths were observed in this study, because

overlapping and non-overlapping crown widths were obtained from field measurements and TLS data respectively.

This study also discussed the influence of number of scans, distance from scanner, cylinder fitting height bin size on the estimation of various parameters. TLS derived measurements underestimated field measurements when the laser pulses had not penetrated completely to the tree crowns due to canopy shadowing. Though an increased amount detail is obtained from two-direction scans, it is time consuming in terms of data collection and processing (Aschoff and Spiecker, 2004; Bienert *et al*., 2006; Dassot *et al*., 2011). Multiple scans should be conducted or correction factors should be applied to reduce the errors in estimation of forest structural parameters. The various metrics derived from TLS point cloud will be useful for inventory and time series analysis.

TLS is a powerful technology that provides highly dense point cloud data, from which various geometric and statistical parameters can be extracted for individual trees (Kankare *et al*., 2013). Since majority of the AGB estimation models are developed only using DBH, we investigated the potential of TLS by extracting various geometric and statistical parameters for AGB estimation. This study presented different methods and statistical approaches to estimate AGB and model the change in AGB using multi-temporal TLS data. The best AGB estimation model for loblolly pines had DBH, height variance, and interquartile distance as independent variables. The best AGB estimation model for hardwoods included volume and crown width as independent variables, both being TLS geometric parameters. Since the mean estimated AGB from the models were not statistically different from the field measured AGB, these models could be used to

obtain non-destructive measurements AGB for loblolly pines and hardwoods. An interesting finding was that AGB estimates for pines obtained from generalized biomass equations and regional biomass equations were not significantly different. Tree shadowing is an important factor that has to be considered and minimized in case of single scan data to prevent the underestimation or overestimation of the derived statistical parameters. For example, 50^{th} percentile or HOME, an important variable used to estimate AGB may be influenced by the laser penetration through the canopy, and the value will be higher in areas where lower portions of the canopy are shadowed due to heavy understory. Multiple scans can be conducted to avoid laser shadows as much as possible due to branches or heavy understory. Co-registered airborne lidar data can also be integrated with terrestrial lidar data to obtain an enhanced characterization of the canopy, which may further prevent the underestimation of certain TLS derived parameters such as tree height, 75^{th} percentile, and 90^{th} percentile. Although we presented methods to estimate AGB only for loblolly pines and hardwoods, they can be applied to other tree species also.

Current and future changes in forest structural parameters and AGB are vital for prudent decision making as well as choosing appropriate growth and yield models. Natural areas can be protected by increasing the yield on fewer acres of natural stands of loblolly pines, thus minimizing the conversion of natural acres to plantations (Bruce and Bailey, 2001). We did not observe a significant relationship between growth in tree height and DBH to field measured heights. Some factors that influenced the growth of loblolly pines were competition due to hardwoods, age of the trees and spacing between

the trees. Regarding AGB change, we did not model the change for hardwoods due to the lack of sufficient trees to develop the model. For AGB change of loblolly pines, approach III (Direct modeling of AGB change with TLS data available for 2009 and 2012) provided the best results. Since the mean estimated AGB changes using the direct modeling approach were not significantly different from the field measured AGB change, forest growth could be studied independent of any field measurements when biomass models are already available. However, the models could be improved by incorporating more trees with a wide range of DBH and tree heights. Negative estimated AGB change using approach I were observed for a few trees (Separate modeling of AGB to estimate AGB change) due to canopy shadowing. The results from approach II (Models developed for 2009 from field and TLS data to estimate biomass in 2012 based on 2012 TLS data only and 2009 biomass models) overestimated the field measured AGB change for most of the trees. Such errors could be minimized by conducting multiple scans. Though a very significant relationship was not observed between the field measured AGB change and TLS estimated AGB change using the three approaches, there are no other studies we can compare results to. An extensive literature review reveals that this is the first study to model the change in AGB using different innovative and conceptual approaches with multi-temporal TLS data.

The results of our study indicate the capability of terrestrial lidar to model the change in tree level forest structural parameters and AGB, with potential for reducing the amount of field work when using multi-temporal terrestrial lidar datasets. To model change in forest structural parameters and AGB at larger scales, multi-stage sampling

could be implemented based on the availability of airborne lidar data. Future work could also investigate the potential of integrating spatially coincident airborne lidar data and terrestrial lidar data to provide an enhanced characterization of the overstory and understory. Reliable information on tree level growth on a larger scale will also be vital to forest fire managers to make critical decisions on clearing the accumulated fuel. Monitoring various forest attributes and biomass using terrestrial and airborne lidar can further be used to validate measurements from imminent spaceborne lidar missions (Dubayah and Drake, 2000; Falkowski *et al*., 2010).

REFERENCES

Applied Imagery, 2010. *Quick Terrain Modeler* (Version 7.1.4) [Software]. Available from http://www.appliedimagery.com/

Aschoff, T., and H. Spiecker, 2004. Algorithms for the automatic detection of trees in laser scanner data. *International Archives of Photogrammetry, Remote Sensing and Spatial Information Sciences*, 36(8) W2: 66 - 70.

Avery, T.E., and H.E. Burkhart, 2002. *Forest Measurements*. 5th ed., New York: McGraw-Hill. 456 p.

Bienert, A., S. Scheller, E. Keane, G. Mullooly, and F. Mohan, 2006. Application of terrestrial laser scanners for the determination of forest inventory parameters. *International Archives of Photogrammetry, Remote Sensing and Spatial Information Sciences*, 36(5) WG3.

Bollandsås, O.M., T.G. Gregoire, E. Næsset, and B.H. Øyen, 2013. Detection of biomass change in a Norwegian mountain forest area using small footprint airborne laser scanner data. *Statistical Methods & Applications*, 22: 113 - 129.

Bortolot, Z.J., and R.H. Wynne, 2005. Estimating forest biomass using small footprint LiDAR data: An individual tree-based approach that incorporates training data. *ISPRS Journal of Photogrammetry & Remote Sensing*, 59: 342 - 360.

Brolly, G., and G. Kiraly, 2009. Algorithms for stem mapping by means of terrestrial laser scanning. *Acta Silvatica et Lignaria Hungarica*, 5: 119 - 130.

Chasmer, L., C. Hopkinson, and P. Treitz, 2006. Investigating laser pulse penetration through a conifer canopy by integrating airborne and terrestrial lidar. *Canadian Journal of Remote Sensing*, *32*(2): 116 - 125.

Chen, Q., P. Gong, D. Baldocchi, and Y.Q. Tian, 2007. Estimating basal area and stem volume for individual trees from lidar data, *Photogrammetric Engineering & Remote Sensing*, 73(12): 1355 - 1365.

Clason, T. R., 1978. Removal of hardwood vegetation increases growth and yield of a young loblolly pine stand. *Southern Journal of Applied Forestry*, 2(3): 96 - 97.

Danson, F.M., D. Hetherington, F. Morsdorf, B. Koetz, and B. Allgower, 2007. Forest canopy gap fraction from terrestrial laser scanning. *Geoscience and Remote Sensing Letters, IEEE*, 4(1): 157 - 160.

Dassot, M., T. Constant, and M. Fournier, 2011.The use of terrestrial LiDAR technology in forest science: application fields, benefits and challenges. *Annals of Forest Science*, 68(5): 959 - 974.

Dean, T. J., and V.C. Baldwin Jr, 1996. Growth in loblolly pine plantations as a function of stand density and canopy properties. *Forest Ecology and Management*, 82(1): 49 - 58.

Drake, J.B., R.O. Dubayah, R.G.Knox, D.B. Clark, and J.B. Blair, 2002. Sensitivity of large-footprint LiDAR to canopy structure and biomass in a neotropical rainforest. *Remote Sensing of Environment*, 81: 378 - 392.

Dubayah, R.O., and J.B. Drake, 2000. Lidar remote sensing for forestry. *Journal of Forestry*, *98*(6): 44 - 46.

Dubayah, R.O., S.L. Sheldon, D.B. Clark, M.A. Hofton, J.B. Blair, G.C. Hurtt, and R.L. Chazdon, 2010. Estimation of tropical forest height and biomass dynamics using lidar remote sensing at La Selva, Costa Rica. *Journal of Geophysical Research: Biogeosciences* (2005-2012), 115(G2).

Evans, D.L., S.D. Roberts, and R.C. Parker, 2006. LiDAR A new tool for forest measurements?. *The Forestry Chronicle*, *82*(2): 211 - 218.

Falkowski M.J., J.S. Evans, S. Martinuzzi, P.E. Gessler, and A.T. Hudak, 2009. Characterizing forest succession with lidar data: An evaluation for the Inland Northwest, USA. *Remote Sensing of Environment*, 113(5): 946 - 956.

Henning, J.G., and P.J. Radtke, 2006. Ground-based laser imaging for assessing three-dimensional forest canopy structure. *Photogrammetric Engineering and Remote Sensing*, 72: 1349 - 1358.

Hopkinson, C., L. Chasmer, C. Young-Pow, and P. Treitz, 2004. Assessing forest metrics with a ground-based scanning lidar. *Canadian Journal of Forest Research*, 34: 573 - 583.

Hopkinson, C., L. Chasmer, and R.J. Hall, 2008. The uncertainty in conifer plantation growth prediction from multi-temporal lidar datasets. *Remote Sensing of Environment*, 112(3): 1168 - 1180.

Houghton, R.A., F. Hall, and S.J. Goetz, 2009. Importance of biomass in the global carbon cycle. *Journal of Geophysical Research: Biogeosciences*, 114(G2).

Huang, H., P. Gong, X. Cheng, N. Clinton, C. Cao, W. Ni, Z. Li, and L. Wang, 2009. Forest structural parameter extraction using terrestrial LiDAR. *Proceedings of Silvilaser2009,* College Station, TX.

Hudak, A. T., J.S. Evans, and A.M. Stuart Smith. 2009. LiDAR utility for natural resource managers. *Remote Sensing*, 1(4): 934 - 951.

Hudak, A.T., E.K. Strand, L.A. Vierling, J.C. Byrne, J.U.H. Eitel, S. Martinuzzi, and M.J. Falkowski, 2012. Quantifying aboveground forest carbon pools and fluxes from repeat LiDAR surveys. *Remote Sensing of Environment*, 123: 25 - 40.

Jenkins, J.C., D.C. Chojnacky, L.S. Heath, and R.A. Birdsey, 2003. National-Scale Biomass Estimators for United States Tree Species. *Forest Science*, 49(1): 12 - 35.

Johnsen, K.H., D. Wear, R. Oren, R.O. Teskey, F. Sanchez, R. Will, J. Butnor, D. Markewitz, D. Richter, T. Rials, H.L. Allen, J. Seiler, D. Ellsworth, C. Maier, G. Katul, and P.M. Dougherty, 2001. Meeting global policy commitments: Carbon sequestration and southern pine forests. *Journal of Forest*, 99 (4):14 - 21.

Kaasalainen, S., J. Hyyppä, M. Karjalainen, A. Krooks, P. Lyytikäinen-Saarenmaa, M. Holopainen, and A. Jaakkola, 2010. Comparison of terrestrial laser scanner and synthetic aperture radar data in the study of forest defoliation. *International Archives of Photogrammetry, Remote Sensing and Spatial Information Sciences*, 38(7A): 82 - 87.

Kankare, V., M. Holopainen, M. Vastaranta, E. Puttonen, X. Yu, J. Hyyppä, M. Vaaja, H. Hyyppä, and P. Alho, 2013. Individual tree biomass estimation using

terrestrial laser scanning. *ISPRS Journal of Photogrammetry and Remote Sensing*, 75: 64 - 75.

Kussner, R., and R. Mosandl, 2000. Comparison of direct and indirect estimation of leaf area index in mature Norway spruce stands of Eastern Germany. *Canadian Journal of Forest Research*, 30(3): 440 - 447.

Lim, K., P. Treitz, M. Wulder, B. St-Onge, and M. Flood, 2003. LiDAR remote sensing of forest structure. *Progress in Physical Geography*, 27: 88 - 106.

Lin, Y., A. Jaakkola, J. Hyyppä, and H. Kaartinen, 2010. From TLS to VLS: Biomass estimation at individual tree level. *Remote Sensing*, 2(8): 1864 - 1879.

Leica Cyclone (Version 7.1.3) [Software]. Available from http://hds.leicageosystems.com/en/Leica-Cyclone_6515.htm

Lefsky, M.A., W.B. Cohen, G.G. Parker, and D.J. Harding, 2002a. Lidar remote sensing for ecosystem Studies. *BioScience*, 52(1): 19 - 30.

Lefsky, M.A., W.B. Cohen, D.J. Harding, G.G Parker, S.A. Acker, and S.T. Gower, 2002b. Lidar remote sensing of above-ground biomass in three biomes. *Global Ecology and Biogeography*, 11(5): 393 - 399.

Lenhart, J.D., T.L. Hackett, C.J. Laman, T.J. Wiswell, and J.A. Blackard, 1987. Tree content and taper functions for loblolly and slash pine trees planted on non-old-fields in east Texas. *Southern Journal of Applied Forestry*, 11(3): 147 - 151.

Loudermilk, E.L., Hiers, J.J. O'Brien, J.J., Mitchell, R.J. Singhania, A., Fernandez, J.C., Cropper, Jr. W.P., and K.C. Slatton, 2009. Ground-based LIDAR: a novel

approach to quantify fine-scale fuelbed characteristics. *International Journal of Wildland Fire*, 18(6): 676 - 685.

Lovell, J.L., D.L.B. Jupp, D.S. Culvenor, and N.C. Coops, 2003. Using airborne and ground-based ranging lidar to measure canopy structure in Australian forests, *Canadian Journal of Remote Sensing*, 29(5): 607 - 622.

Maas, H.-G. Bienert, A., S. Scheller, and E. Keane, 2008. Automatic forest inventory parameter determination from terrestrial laser scanner data, *International Journal of Remote Sensing*, 29(5): 1579 - 1593.

Miller, J. H., Zutter, B.R., Zedaker, S.M., Edwards, M.B., Haywood, J.D., and R.A. Newbold, 1991. A regional study on the influence of woody and herbaceous competition on early loblolly pine growth. *Southern Journal of Applied Forestry*, 15(4): 169 - 179.

Moskal, L.M., T. Erdody, A. Kato, J. Richardson, G. Zheng, and D. Briggs, 2009. LiDAR Applications in Precision Forestry. *Proceedings of Silvilaser2009*. College Station, TX.

Moskal, L.M., and G. Zheng, 2012. Retrieving Forest Inventory Variables with Terrestrial Laser Scanning (TLS) in Urban Heterogeneous Forest. *Remote Sensing*, 4: 1 - 20.

McGaughey, R.J, 2007. *FUSION/LDV*: software for LIDAR data analysis and visualization. USDA Forest Service. Pacific Northwest Research Station, 28 - 30.

Næsset, E., T. Gobakken, J. Holmgren, H. Hyyppä, J. Hyyppä, M. Maltamo, M. Nilsson, H. Olsson, A. Persson, and U. Söderman, 2004. Laser scanning of forest

resources: the Nordic experience. *Scandinavian Journal of Forest Research*, 19(6): 482 - 489.

Næsset, E., T. Gobakken, S. Solberg, T.G. Gregoire, R. Nelson, G. Ståhl, and D. Weydahl, 2011. Model-assisted regional forest biomass estimation using LiDAR and InSAR as auxiliary data: A case study from a boreal forest area. *Remote Sensing of Environment*, 115(12): 3599 - 3614.

Næsset, E., O.M. Bollandsås, T. Gobakken, T.G. Gregoire, and G. Ståhl, G, 2013. Model-assisted estimation of change in forest biomass over an 11year period in a sample survey supported by airborne LiDAR: A case study with post-stratification to provide "activity data". *Remote Sensing of Environment*, 128, 299 - 314.

Popescu, S.C., R.H. Wynne, and R.F. Nelson, 2003. Measuring individual tree crown diameter with lidar and assessing its influence on estimating forest volume and biomass. *Canadian Journal of Remote Sensing*, 29(5): 564 - 577.

Popescu, S.C., 2007. Estimating biomass of individual pine trees using airborne LiDAR, *Biomass and Bioenergy*, 31(9): 646 - 655.

Popescu, S.C., and K. Zhao, 2008. A voxel-based lidar method for estimating crown base height for deciduous and pine trees. *Remote Sensing of Environment*, 112(3): 767 - 781.

Pueschel, P., G. Newnham, G. Rock, T. Udelhoven, W. Werner, and J. Hill, 2013. The influence of scan mode and circle fitting on tree stem detection, stem diameter

and volume extraction from terrestrial laser scans. *ISPRS Journal of Photogrammetry and Remote Sensing*, 77: 44 - 56.

Stukey, J. D, 2013. Deriving a framework for estimating individual tree measurements with Lidar for use in the TAMBEETLE southern pine beetle infestation growth model (*Master's Thesis*), Texas A&M University, College Station, TX.

Tansey, K., N. Selmes, A. Anstee, N.J. Tate, and A. Denniss, 2009. Estimating tree and stand variables in a Corsican Pine woodland from terrestrial laser scanner data. *International Journal of Remote Sensing*, 30(19): 5195 - 5209.

Thies, M., and H. Spiecker, 2004. Evaluation and future prospects of terrestrial laser scanning for standardized forest inventories. *Proceedings of ISPRS Workshop Laser-Scanners for Forest and Landscape Assessment*, Freiburg, Germany, 192 - 197.

Van der Zande, D., W. Hoet, I. Jonckheere, J. Van Aardt, and P. Coppin, 2006. Influence of measurement set-up of ground-based LiDAR for derivation of tree structure. *Agricultural and Forest Meteorology*, 141(2): 147 - 160.

Van Leeuwen, M., and M. Nieuwenhuis, 2010. Retrieval of forest structural parameters using LiDAR remote sensing. *European Journal of Forest Research*, 129(4): 749 - 770.

Watt, P.J., and D.N.M. Donoghue, 2005. Measuring forest structure with terrestrial laser scanning. *International Journal of Remote Sensing*, 26(7): 1437 - 1446.

Wezyk, P., K. Koziol, M. Glista, and M. Pierzchalski, 2007. Terrestrial laser scanning versus traditional forest inventory. First results from the Polish forests.

International Archives of Photogrammetry, Remote Sensing and Spatial Information Science, 36(3) W52: 424 - 429.

Williams, M.S., W.A. Bechtold, and V.J. LaBau, 1994. Five instruments for measuring tree height: An evaluation. *Southern Journal of Applied Forestry,* 18(2): 76 - 82.

Yao, T., X. Yang, F. Zhao, Z. Wang, Q. Zhang, D. Jupp, J. Lovell, D. Culvenor, G. Newnham, W. Ni-Meister, C. Schaaf, C. Woodcock, J. Wang, X. Li, and A. Strahler, 2011. Measuring forest structure and biomass in New England forest stands using Echidna ground-based lidar. *Remote Sensing of Environment*, 115(11): 2965 - 2974.

Yu, X., J. Hyyppä, A. Kukko, M. Maltamo, and H. Kaartinen, 2006. Change detection techniques for canopy height growth measurements using airborne laser scanner data. *Photogrammetric Engineering and Remote Sensing*, 72: 1339 - 1348.

Zhao, K., D. Valle, S.C. Popescu, X. Zhang, and B. Mallik, 2013. Hyperspectral remote sensing of plant biochemistry using Bayesian model averaging with variable and band selection. *Remote Sensing of Environment,* 132: 102 - 119.

Zolkos, S.G., S.J. Goetz, and R. Dubayah, 2013. A meta-analysis of terrestrial aboveground biomass estimation using lidar remote sensing, *Remote Sensing of Environment*, 128: 289 - 298.